lines and mouse models have shown that the progression to CRPC could be associated with enhanced AR expression, as indicated by findings from AR down-regulation using dominant-negative AR mutants, small interfering RNA (siRNA), or small molecules, whereas increased AR expression converts androgen-dependent PCa cells to CRPC (7–10). The *AR* gene is overexpressed in most CRPCs, 10–20% of which show amplification of the *AR* gene (11). Also, less than 10% of CRPCs were found to have somatic mutations in the *AR* gene, which could confer promiscuous activity to the receptor, allowing its activation by nonandrogen steroids and antiandrogens (12). Furthermore, the AR pathway in CRPC was considered to rely on changes in expression of growth factors, such as IGF (13), HER-2 (14), and IL-6 (15), which could modify AR activity. Also, AR signaling could be modulated by AR cofactors such as heat-shock protein 27 (Hsp27) (16), peroxiredoxin1 (17), Tip60, histone deacetylase 1 (HDAC1) (18), ARA 54 (19), ARA55 (20), ARA70 (21), GRIP1 (22), HMGB1, HMGB2 (23), PIAS1, PIAS3 (24), and SRC1 (25), some of which have been reported to be implicated in CRPC. Modification of these growth factors and cofactors in CRPC may cause androgen-dependent PCa to gain castration-resistant status.

Peroxisome proliferator-activated receptor γ (PPARγ) coactivator-1α (PGC-1α) was isolated based on its abilities to interact with PPARγ in a two-hybrid screening system and to enhance glucocorticoid responses in a functional genetic screening system (26, 27). It has previously been shown that PGC-1α has a novel role in adaptive thermogenesis, where it enhances the ability of PPARγ and nuclear respiratory factors (NRF1 and NRF2) to induce the synthesis of the enzymes required for oxidative metabolism (28). PGC-1α has been shown to be expressed and highly regulated in brown adipose tissue and skeletal muscle (26). Also, PGC-1α is expressed in the heart, kidney, and brain, suggesting that it is involved in processes other than thermogenesis (26). Because AR is also expressed in these tissues, we hypothesized that PGC-1α might have a role in various tissues together with AR. PGC-1α is known to interact with and enhance the transactivation of other nuclear receptors such as estrogen receptor α (ERα) (29, 30). Also, PGC-1α interacts with and activates ERα and ERβ in a ligand-independent manner with a particularly high-binding affinity to ERβ (31). In contrast, PGC-1β, also known as PERC, selectively binds to ERα in a ligand-dependent manner and activates its transcriptional ability (29, 32). Similar to a relationship between androgen and AR in carcinogenesis and development of PCa, a relationship between estrogen and ER has also been established, and it was reported that reduced levels of ovarian steroids and ERα significantly decrease the breast cancer risk (33, 34). Furthermore, antiestrogen therapies that inhibit estrogen synthesis or block ER activity are used to treat breast cancer similar to antiandrogen agents to treat PCa. Wirtenberger *et al.* (35) recently showed that a polymorphism of PGC-1α was associated with familial breast cancer, high-risk familial breast cancer, and bilateral familial breast cancer.

However, the function of PGC-1α in association with AR and in the progression of CRPC currently remains unknown. In this study, we intended to resolve the function of PGC-1α in association with AR and PCa. Our data showed that PGC-1α interacted with AR and was involved in the proliferation of androgen-dependent and CRPC cells. Together, PGC-1α appears to be a key factor involved in the progression to PCa, and is a promising molecular target for treating PCa, even CRPC.

Results

PGC-1α interacts with AR *in vitro* and *in vivo*

We intended to research the mechanisms responsible for carcinogenesis and progression of PCa in terms of AR function. Accordingly, we found that PGC-1α might interact with AR. First, the interaction between AR and PGC-1α was investigated by a glutathion S-transferase (GST) pull-down assay using GST-fused AR and Myc-Flag-tagged PGC-1α proteins. As shown in Fig. 1A, Myc-Flag-tagged PGC-1α was found to interact with GST-AR. To confirm this finding, a coimmunoprecipitation assay using the overexpression method was performed. PC-3 cells, which expressed no AR mRNA and protein, were transfected with GFP-tagged AR and Myc-Flag-tagged PGC-1α expression plasmids, and a coimmunoprecipitation assay was performed. Myc-Flag-tagged PGC-1α reproducibly interacted with the GFP-tagged AR protein. Simultaneously, we assayed whether the interaction between PGC-1α and AR could be influenced by dihydrotestosterone (DHT). PC-3 cells were transfected with the GFP-tagged AR and Myc-Flag-tagged PGC-1α expression plasmids, and then cultured under charcoal-stripped medium with or without DHT. The results of the coimmunoprecipitation assay showed that DHT did not influence this interaction (Fig. 1B). Last, we investigated whether endogenous proteins interacted with each other. Using cellular extracts of LNCaP cells expressing AR protein that were cultured under charcoal-stripped medium with or without DHT, the endogenous AR was immunoprecipitated using anti-AR antibody, and the immunoprecipitated samples were blotted with anti-PGC-1α antibody. As expected, endogenous AR interacted with PGC-1α, and reproducibly, this interaction was not affected by DHT (Fig. 1C).

Downloaded from mend.endojournals.org at Kyushu Univ 00A Central Lib on February 16, 2010

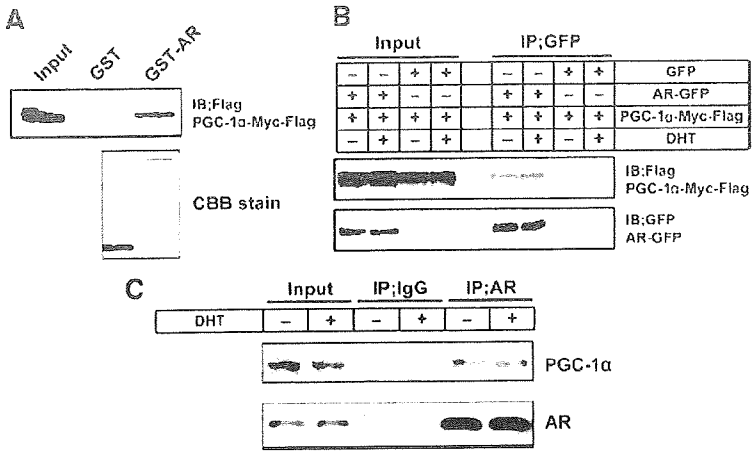

FIG. 1. PGC-1α interacts with AR *in vitro* and *in vivo*. A, Equal amounts of GST and GST-AR fusion proteins were immobilized on glutathione-sepharose 4B and were incubated with nuclear extracts from PC-3 cells transfected with PGC-1α-Myc-Flag plasmid. The bound protein and 10% of the input were subjected to SDS-PAGE, and Western blot analysis was performed using the anti-Flag antibody. Purified GST and GST-AR fusion proteins stained with Coomassie Brilliant Blue (CBB; Wako, Osaka, Japan) are also shown. B, PC-3 cells were cotransfected with 1.0 μg of each of the indicated expression plasmids and incubated in charcoal-stripped medium with or without 10 nM of DHT. Whole-cell extracts (300 μg) were immunoprecipitated with agarose-conjugated anti-GFP antibody. The resulting immunocomplexes and whole-cell extracts (30 μg) were subjected to SDS-PAGE, and Western blot analysis was performed using anti-Flag and anti-GFP antibodies. C, Whole-cell extracts (500 μg) were prepared from LNCaP cells incubated in charcoal-stripped medium with or without 10 nM of DHT and were immunoprecipitated (IP) with 2.0 μg of rabbit IgG or anti-AR antibody (C-19) and 20 μl of protein A/G agarose. The resulting immunocomplexes and whole-cell extracts (50 μg) were subjected to SDS-PAGE, and Western blot analysis was performed using anti-PGC-1α and anti-AR (C-19) antibodies.

PGC-1α is overexpressed in PCa cells and PGC-1α knock-down reduces PSA expression

To investigate a role of PGC-1α in PCa, we examined PGC-1α expressions in human normal prostate epithelial cells (RWPE-1 cells) and a panel of PCa cells (DU145, PC-3, VCaP, 22Rv1, LNCaP, and castration-resistant LNCaP derivatives CxR cells). PGC-1α was overexpressed in PCa cells compared with that in normal prostate epithelial cells. Also, PGC-1α expression level was similar between LNCaP and CxR cells (Fig. 2A). Furthermore, PGC-1α expression was not affected by DHT in LNCaP and CxR cells (Fig. 2B). To confirm the function of PGC-1α on AR, we next examined the expression of a well-known AR target gene, PSA, after knock-down of PGC-1α. After LNCaP and CxR cells were transfected with PGC-1α-specific siRNAs, quantitative real-time PCR and Western blot analysis for PSA were performed. The results showed that the expression of PSA mRNA was decreased by PGC-1α knock-down in the presence of DHT, although basal PSA expression was decreased by androgen starvation, but not in the absence of DHT. In addition, PSA mRNA expression level both in the presence or absence of DHT was decreased after PGC-1α knock-down also in CxR cells (Fig. 2C), in which AR could locate in nucleus and have a potential to transactivate its target genes even without ligand (Shiota, M., A. Yokomizo A., D. Masubichi, Y. Tuda, J. Inokuchi, M.Eto, T. Uchiumi, N. Fujimoto, S. Naito, manuscript submitted). Similar findings in terms of the protein PSA level were obtained when androgen-dependent LNCaP cells and CxR cells were transfected with PGC-1α-specific siRNAs. Also, transfection efficiencies of PGC-1α-specific siRNAs seemed to be equivalent between LNCaP and CxR cells as indicated by decrease of PGC-1α protein expression. Furthermore, as previously reported, the expression of AR was increased in the CxR cells compared with that in the parental LNCaP cells (Fig. 2D) (9–11).

PGC-1α activates AR transcriptional activity

Because PGC-1α was thought to interact with AR and regulate PSA expression, we determined the effect of PGC-1α on AR transcriptional activity using a luciferase assay. First, the PC-3 cells were transfected with a PSA reporter plasmid, pGLPSAp5.8, possessing PSA enhancer and promoter regions (~5.8 kb) with three putative androgen-responsive elements (AREs) and a PGC-1α expression plasmid in addition to pCMV-AR expressing wild-type AR protein. Without DHT, luciferase activity was hardly detected even with PGC-1α overexpression. However, luciferase activity was significantly increased with DHT. Also, PGC-1α overexpression increased the transcriptional activity of PSA. In PCa, several AR mutations such as T887A in LNCaP cells have been found. Simultaneously, we investigated whether the AR mutation influences the PGC-1α function as a coactivator of AR in PC-3 cells. PGC-1α overexpression enhanced luciferase activity of PSA reporter plasmid even when mutated AR (T887A) was expressed in the PC-3 cells. Next, mouse mammary tumor virus (MMTV)-Luc possessing an MMTV promoter region with a putative ARE was used, and similar results were obtained. PGC-1α overexpression increased the transcriptional activities of MMTV when DHT was applied in addition to AR expression (Fig. 3A). Last, to confirm the above results, a knock-down assay using PGC-1α-specific siRNAs was performed. As expected, PGC-1α knock-down decreased the luciferase activity of the PSA and MMTV reporter plasmids to approximately 10–40% in LNCaP cells with DHT, whereas basal luciferase activity without DHT was not affected by PGC-1α

Downloaded from mend.endojournals.org at Kyushu Univ 00A Central Lib on February 16, 2010

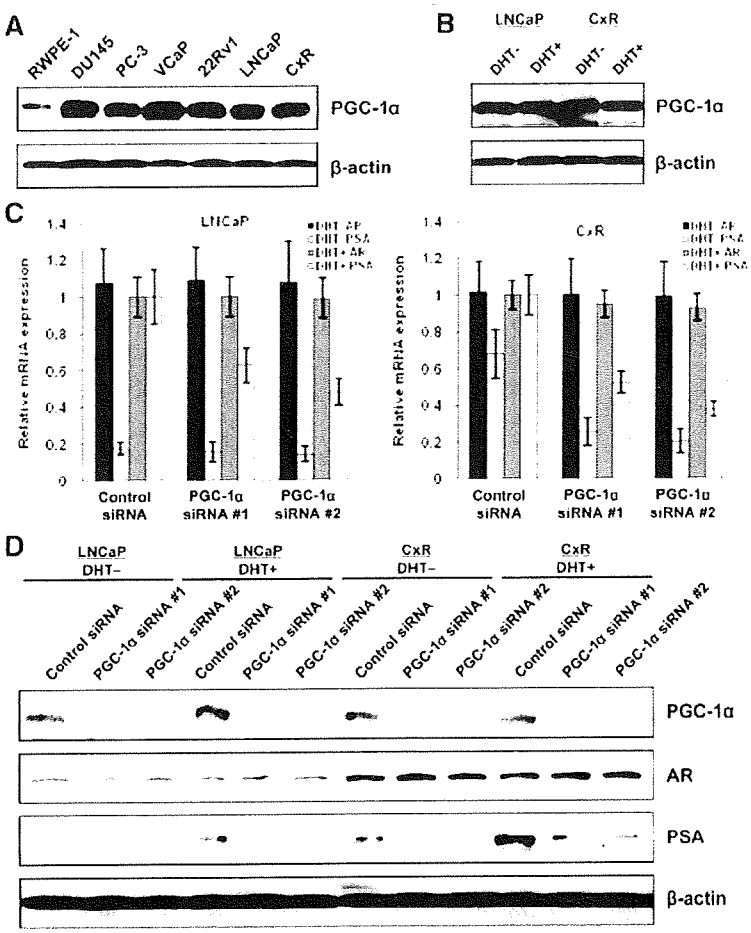

FIG. 2. PGC-1α is overexpressed in PCa cells and PGC-1α knock-down reduces PSA expression. A, Whole-cell extracts from the indicated cells were subjected to SDS-PAGE, and Western blot analysis was performed using anti-PGC-1α and anti-β-actin antibodies. B, Whole-cell extracts from LNCaP, CxR cells incubated in charcoal-stripped medium with or without 10 nM of DHT for 72 h were subjected to SDS-PAGE, and Western blot analysis was performed using anti-PGC-1α and anti-β-actin antibodies. C, LNCaP and CxR cells were transfected with 50 nM of control siRNA, PGC-1α siRNA no. 1 or PGC-1α siRNA no. 2, and incubated in charcoal-stripped medium with or without 10 nM of DHT for 72 h. After extraction of total RNA and synthesis of cDNA, quantitative real-time PCR was performed using the primers and probes for AR, PSA, and GAPDH. The transcription levels of AR and PSA were corrected for the corresponding GAPDH transcript level. All values represent at least three independent experiments. The level of each transcript from cells transfected with control siRNA and incubated with DHT corresponds to 1. *Boxes*, Mean; *bars*, ± SD. D, Whole-cell extracts from cells prepared in C were subjected to SDS-PAGE, and Western blot analysis was performed using anti-PGC-1α, anti-AR (C-19), anti-PSA, and anti-β-actin antibodies.

knock-down (Fig. 3B). These results indicate that PGC-1α can affect PSA transcription androgen/AR signaling-dependently.

N-terminal domain (NTD) of PGC-1α interacts with the N-terminal transactivation domain (TAD) of AR

The finding that PGC-1α interacted with AR and had a functional role with AR prompted us to examine which domains are involved. First, a GST pull-down assay was performed using GST-AR and its series of deletion mutants with Myc-Flag-tagged PGC-1α (Fig. 4A). As shown in Fig. 4B, PGC-1α interacted with the TAD of AR. Next, GST-PGC-1α and its series of deletion mutants were used for the GST pull-down assay with nuclear extracts of LNCaP (Fig. 4C). As shown in Fig. 4D, AR interacted with the NTD of PGC-1α.

TAD of AR is indispensable for augmentation of AR-transcriptional activity by PGC-1α

Because PGC-1α was found to interact with the TAD of AR, we investigated whether the transcriptional ability of TAD-deleted AR was affected by PGC-1α manipulation. First, we constructed an AR-GFP 508-920 plasmid expressing GFP-tagged TAD-deleted AR protein. It is known that the TAD of AR interacts with a C-terminal ligand-binding domain (LBD) and can form a homodimer in a head-to-tail fashion binding to the ARE drive the expression of its target genes (36). Therefore, a coimmunoprecipitation assay was performed using AR-GFP 508-920 and PGC-1α-Myc-Flag expression plasmids in LNCaP cells. An interaction between AR-GFP 508-920 and endogenous AR protein was found to be augmented by PGC-1α expression, probably through an interaction between the LBD of AR-GFP 508-920 and the TAD of endogenous AR (Fig. 5A). To confirm augmentation of an interaction between TAD and LBD of AR, we constructed pCMV-AR 1-567 plasmid expressing LBD− and most part of DBD-deleted AR protein, and performed coimmunoprecipitation assay using PC-3 cells transfected with AR-GFP 508-920, pCMV-AR 1-567, and PGC-1α-Myc-Flag expression plasmids. The result clearly showed that PGC-1α expression increased an interaction between TAD and LBD of AR (Fig. 5B). Then, a luciferase reporter assay was performed to confirm the effects of PGC-1α against AR-GFP 508-920. Although the transcription of PSA was increased in PC-3 cells transfected with the PGC-1α-Myc-Flag expression plasmid, full-length AR-GFP expression plasmid, and PSA reporter plasmid, the transcriptional ability of AR-GFP 508-920 was not affected by PGC-1α expression (Fig. 5C). Similar results were obtained when the MMTV-reporter plasmid was used (Fig. 5D).

Knock-down of PGC-1α decreases the DNA-binding ability of AR

Disruption of the interaction between the TAD and LBD of AR has a potential to inhibit the DNA binding ability of AR (37, 38). Because PGC-1α interacted with

Downloaded from mend.endojournals.org at Kyushu Univ 00A Central Lib on February 16, 2010

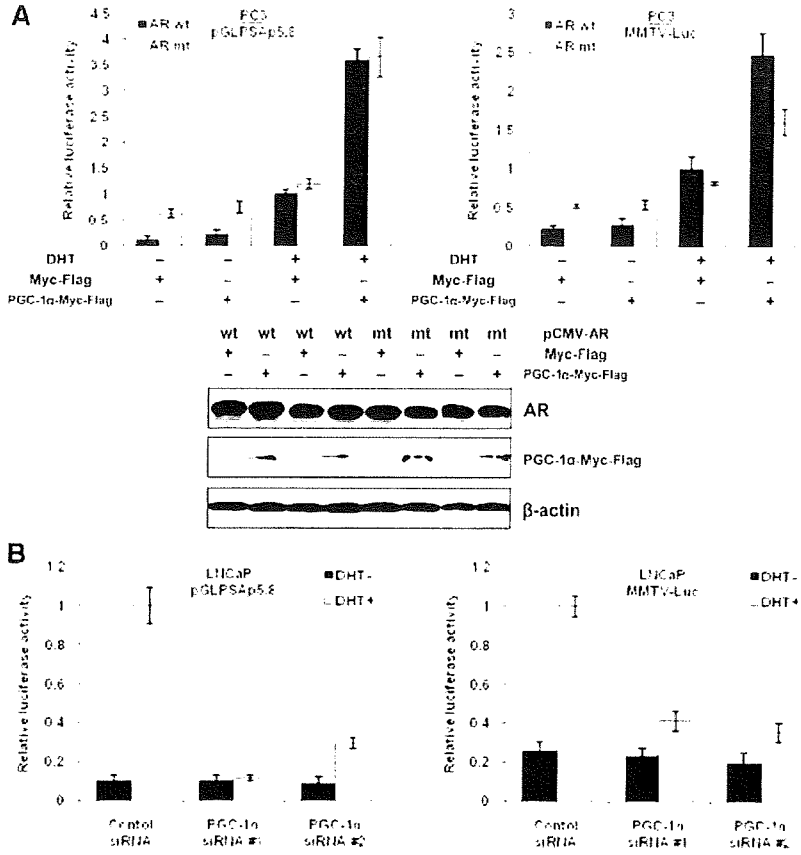

FIG. 3. PGC-1α activates transcriptional activity of AR. A, PC-3 cells were transiently transfected with 0.33 μg of the indicated reporter plasmids, 0.33 μg of Myc-Flag or PGC-1α-Myc-Flag, 0.33 μg of the pCMV-AR [wildtype (wt)] or pCMV-ARmut877 [mutant (mt)], and 0.05 μg of pRL-TK, and incubated in charcoal-stripped medium with or without 10 nM of DHT for 48 h. *Firefly* luciferase activity was corrected for the corresponding *Renilla* luciferase activity. All values represent at least three independent experiments. The luciferase activity of each reporter plasmid with the pCMV-AR and Myc-Flag expression plasmids transfection incubated in charcoal-stripped medium with DHT corresponds to 1. *Boxes*, Mean; *bars*, ± SD. Whole-cell extracts from PC-3 cells transfected with 0.33 μg of each of the indicated plasmids were subjected to SDS-PAGE, and Western blot analysis was performed using anti-Flag, anti-AR (C-19), and anti-β-actin antibodies. B, LNCaP cells were transiently transfected with 20 nM of control siRNA, PGC-1α siRNA no. 1 or PGC-1α siRNA no. 2, followed by transfection with 0.5 μg of the indicated reporter plasmid and 0.05 μg of pRL-TK at intervals of 12 h, and incubated in charcoal-stripped medium with or without 10 nM of DHT. The luciferase assay was performed as described in A. The luciferase activity of each reporter plasmid with control siRNA transfection incubated in charcoal-stripped medium with DHT corresponds to 1. *Boxes*, mean; *bars*, ± SD.

the TAD of AR and was involved in the interaction between the TAD and the LBD of AR, we investigated whether the DNA binding ability of AR was affected by PGC-1α manipulation. The PSA enhancer and promoter regions contained three AREs known as ARE I, ARE II, and ARE III (Fig. 6A). When the samples from LNCaP cells immunoprecipitated with anti-AR antibody were amplified using ARE-containing primer pairs, PCR products were abundant when the primer pairs A/B, C/D, and G/H were used, but not when the primer pairs E/F and I/J were used. Also, the binding of AR to ARE was decreased by the withdrawal of androgen (39) according to withdrawal duration. Similar to a previous report that AR gradually dissociated with DHT and exported to cytoplasm by androgen withdrawal (40), androgen withdrawal for 4 and 16 h reduced AR binding to PSA A/B, C/D, and G/H by approximately 30 and 60%, respectively. Furthermore, when PGC-1α expression was down-regulated by transfecting LNCaP cells with PGC-1α-specific siRNAs, the binding of AR to ARE within the PSA enhancer and promoter regions was reduced (Fig. 6B). These results were confirmed using conventional PCR method (see supplemental Fig. 1A published as supplemental data on The Endocrine Society's Journals Online web site at http://mend.endojournals.org). Similar results were obtained also in CxR cells by both quantitative real-time PCR and conventional PCR methods, although AR binding to ARE in CxR cells was less affected by androgen deprivation (Fig. 6C and supplemental Fig. 1B).

Knock-down of PGC-1α represses cell proliferation in androgen-dependent and CRPC cells

The finding that PGC-1α was involved in a regulation of transcriptional activity of AR prompted us to examine whether PGC-1α might affect the proliferation of PCa cells through modulation of AR function. First, we investigated the proliferation of LNCaP cells transfected with PGC-1α-specific siRNAs in medium containing 1 nM or 10 nM of DHT, or not containing. When PGC-1α was knocked down, cell proliferations in both media were significantly reduced in the presence of DHT, but not in the absence of DHT (Fig. 7A). These results were similar to those with AR knock-down (data not shown). To clarify the mechanism of cell growth retardation by PGC-1α knock-down, we performed flow cytometry analysis for cell-cycle analysis. As shown in Fig. 7B, androgen deprivation induced cell-cycle arrest at G_1 phase. Also, PGC-1α knock-down in medium containing 1 nM or 10 nM of DHT induced cell-cycle arrest at the G_1 phase, but not in medium not containing DHT similar to that with AR knock-down (data not shown); thus, decreasing cell proliferation. However, PGC-1α knock-down in CRPC

Downloaded from mend.endojournals.org at Kyushu Univ 00A Central Lib on February 16, 2010

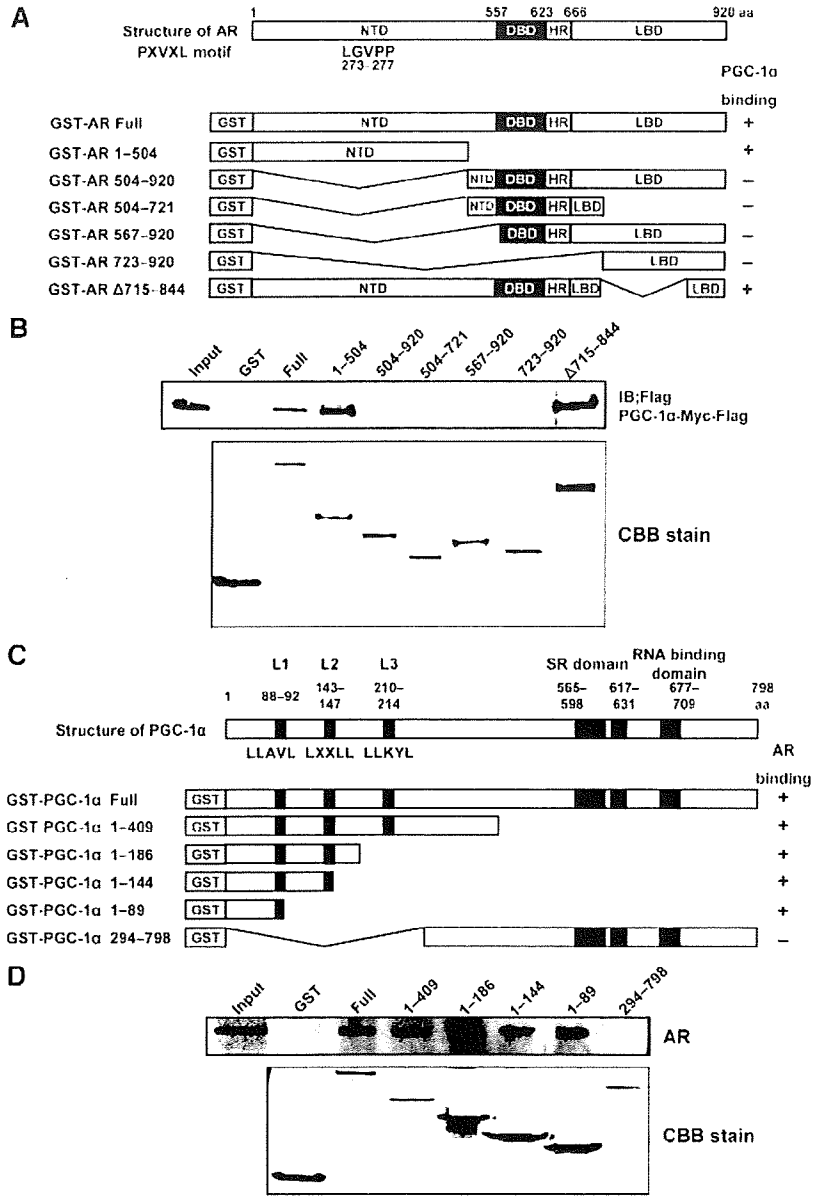

FIG. 4. The NTD of PGC-1α interacts with the TAD of AR. A, Schematic representation of the GST-AR deletion mutants. B, Equal amounts of GST, GST-AR, and various GST-AR deletion mutant fusion proteins, as shown in A, were immobilized on glutathione-sepharose 4B and were incubated with nuclear extracts from PC-3 cells transfected with PGC-1α-Myc-Flag expression plasmid. The bound protein samples and 10% of the input were subjected to SDS-PAGE, and Western blot analysis was performed using an anti-Flag antibody. Purified GST, GST-AR, and GST-AR deletion mutant fusion proteins stained with CBB are also shown. C, Schematic representation of GST-PGC-1α deletion mutants. D, Equal amounts of GST, GST-PGC-1α, and various GST-PGC-1α deletion mutant fusion proteins shown in C, immobilized on glutathione-sepharose 4B, were incubated with nuclear extracts from LNCaP cells. Bound protein samples and 10% of input were subjected to SDS-PAGE, and Western blot analysis was performed using an anti-AR antibody (C-19). Purified GST, GST-PGC-1α, and GST-PGC-1α deletion mutant fusion proteins stained with Coomassie Brilliant Blue (CBB) are also shown. IB, Immunoblots.

cells with no AR expression, PC-3 cells, affected cell proliferation to a lesser extent than that in LNCaP cells. In addition, under androgen starvation, the growth of PC-3 cells was similar to that in medium containing androgens. When PGC-1α was knocked down, PC-3 cell growth in the androgen-deficient medium was similar to that in androgen-containing medium (Fig. 7C). CxR cells are derived from LNCaP cells and exhibit high expression of AR proteins compared with their parental cells, as shown in Fig. 2D. Overexpression of AR has been thought to promote CRPC cell growth, even under androgen starvation by augmentation of AR signaling. Because CxR cells exhibit enhanced AR expression, blockade of AR signaling may be effective to inhibit cell proliferation in CxR cells. As expected, PGC-1α knock-down in CxR delayed cell growth slightly more effectively than that in parental LNCaP cells, most likely by blocking AR signaling both in the absence and presence of DHT (Fig. 7D).

Discussion

Coactivators can interact with and enhance the transcriptional activity of ligand-bound or ligand-unbound AR, and some coactivators are overexpressed in PCa, suggesting that coactivators of AR might be involved in prostate carcinogenesis (41, 42). Various studies have shown that steroid receptors, particularly AR, have pivotal roles in all stages of prostate carcinogenesis (3, 43). Because the activity of steroid receptors is potentiated by a variety of coactivators, it is reasonable to believe that these proteins may also be involved in prostate carcinogenesis (44, 45). Indeed, recent studies have shown that the mRNA of some steroid receptor coactivators is overexpressed in PCa tissues and cell lines (46). The first *bona fide* steroid hormone receptor coactivator, SRC-1, was identified by virtue of its ability to interact with the hormone binding domain of agonist-activated progesterone receptor (47). Subsequently, it was shown that SRC-1 was able to interact efficiently with most nuclear receptors. SRC-3 was first isolated as a steroid receptor coactivator. Recently, it was reported that SRC-3 was overexpressed in PCa spec-

Downloaded from mend.endojournals.org at Kyushu Univ 00A Central Lib on February 16, 2010

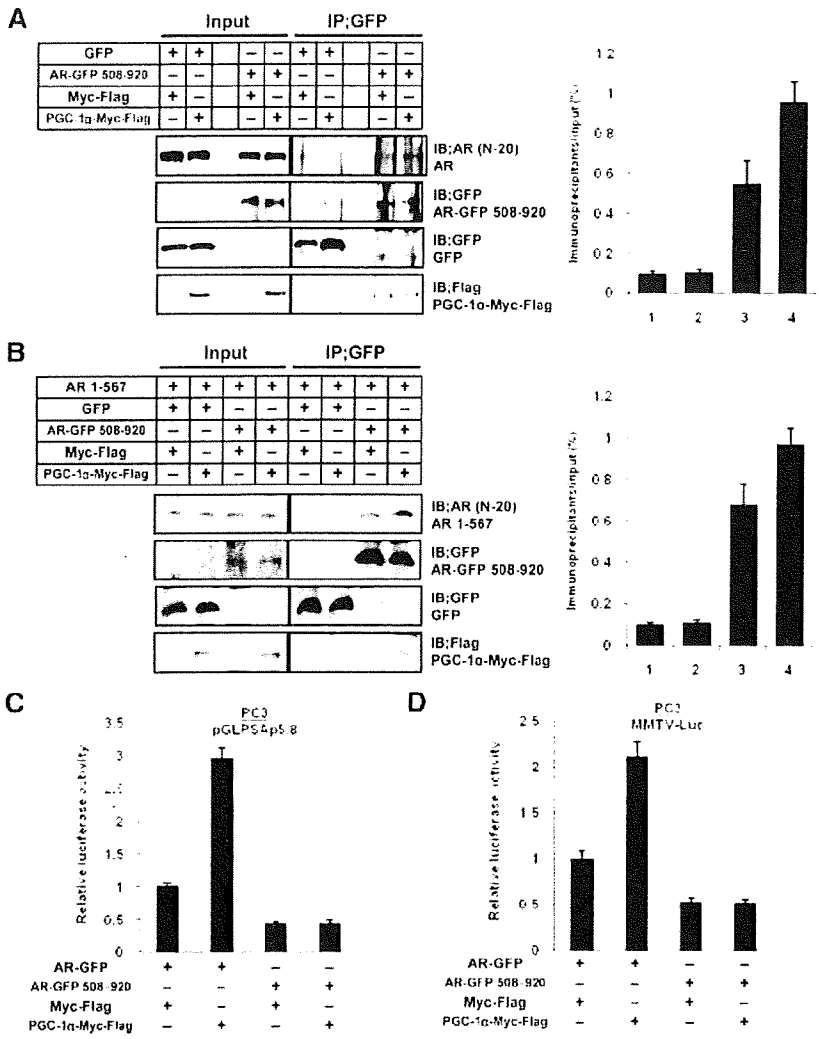

FIG. 5. The TAD of AR is indispensable for the augmentation of AR transcriptional activity by PGC-1α. A, LNCaP cells were cotransfected with 1.0 μg of each of the indicated expression plasmids and were incubated for 48 h. Whole-cell extracts (300 μg) were immunoprecipitated (IP) with agarose-conjugated anti-GFP antibody. The resulting immunocomplexes and whole-cell extracts (30 μg) were subjected to SDS-PAGE, and Western blot analysis was performed using anti-AR (N-20), anti-GFP, and anti-Flag antibodies. The signal intensities for AR protein of coimmunoprecipitated samples were corrected for the results of the corresponding preimmunoprecipitated samples. All values represent at least three independent experiments. Lane 1, GFP and Myc-Flag; lane 2, GFP and PGC-1α-Myc-Flag; lane 3, AR-GFP 508-920 and Myc-Flag; lane 4, AR-GFP 508-920 and PGC-1α-Myc-Flag. *Boxes*, mean; *bars*, ± SD. B, PC-3 cells were cotransfected with 0.65 μg of each of the indicated expression plasmids and were incubated for 48 h. Coimmunoprecipitation assay and Western blot analysis were performed as described in A. The signal intensities for AR 1-567 protein of coimmunoprecipitated samples were corrected for the results of the corresponding preimmunoprecipitated samples. All values represent at least three independent experiments. Lane 1, GFP and Myc-Flag; lane 2, GFP and PGC-1α-Myc-Flag; lane 3, AR-GFP 508-920 and Myc-Flag; lane 4, AR-GFP 508-920 and PGC-1α-Myc-Flag. *Boxes*, Mean; *bars*, ± SD. C and D, PC-3 cells were transiently transfected with 0.33 μg of pGLPSAp5.8 (C) or MMTV-Luc (D), 0.33 μg of Myc-Flag or PGC-1α-Myc-Flag, 0.33 μg of the AR-GFP or AR-GFP 508-920, and 0.05 μg of pRL-TK and incubated in charcoal-stripped medium with 10 nM of DHT for 48 h. *Firefly* luciferase activity was corrected for the corresponding *Renilla* luciferase activity. All values represent at least three independent experiments. The luciferase activity of each reporter plasmid with the AR-GFP and Myc-Flag expression plasmids transfection corresponds to 1. *Boxes*, mean; *bars*, ± SD. IB, Immunoblots.

imens, and its overexpression was correlated with PCa proliferation and is inversely correlated with apoptosis (48). AR coactivators are also involved in castration-resistant progression of PCa, which is critical for advanced PCa patients (49, 50). In this study, PGC-1α was revealed to be overexpressed in PCa cells.

PGC-1α was originally identified as a transcriptional coactivator of PPARγ, and it was determined that PGC-1α also interacts with other nuclear receptors (26, 29). These findings suggest that PGC-1α might also interact with AR and may be involved in carcinogenesis and the progression to CRPC. Therefore, we investigated the interaction between PGC-1α and AR using a GST pull-down assay *in vitro* and coimmunoprecipitation assay *in vivo*. As expected, PGC-1α interacted with AR, and enhanced the transcriptional activity of AR target genes, PSA, and MMTV. Also, we determined the regions of PGC-1α and AR that interact with each other. The results indicate that the NTD of PGC-1α interacts with the TAD of AR. The NTD of PGC-1α contains three LXXLL-like motifs resembling an LXXLL motif, which is known to mediate the recruitment of the p160-type of coactivators to nuclear receptors (51). Mutations of LXXLL motif have been shown to disrupt its interactions with nuclear receptors and abolish its coactivator function (51–53). However, our result showed that deletion mutant of PGC-1α (GST-PGC-1α 1-89) not containing complete LXXLL motif could also interacted with AR. This result indicates that LXXLL motif may be unnecessary for PGC-1α to interact with AR. Otherwise, LL portion (amino acids 88-89) of LXXLL motif may be sufficient to interact with AR.

After determining the region of PGC-1α that interacts with AR, we investigated the region of AR that interacts with PGC-1α. It was shown that PGC-1α interacts with the hinge region or the NTD of nuclear receptors, but

Downloaded from mend.endojournals.org at Kyushu Univ 00A Central Lib on February 16, 2010

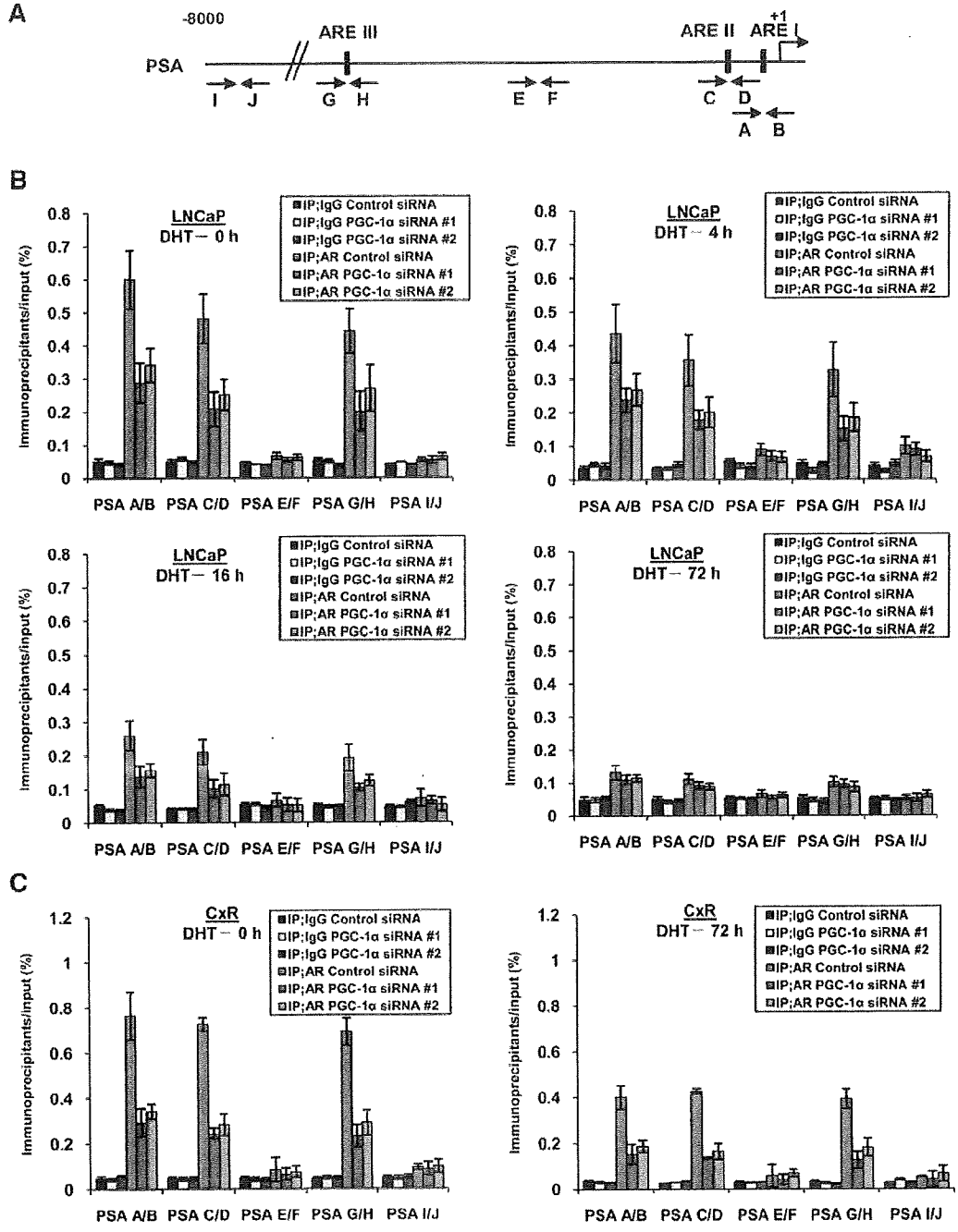

FIG. 6. Knock-down of PGC-1α decreases the DNA-binding ability of AR. A, *Black boxes* and *black arrows* indicate the AREs and PCR primer regions, respectively. B and C, LNCaP (B) and CxR (C) cells were transfected with 50 nM of control siRNA, PGC-1α siRNA no. 1 or PGC-1α siRNA no. 2, and incubated for 72 h. The medium was exchanged from charcoal-stripped medium with 10 nM of DHT into medium without DHT at the indicated time before harvest. The nuclear extracts were then immunoprecipitated (IP) with 2.0 μg of rabbit IgG or anti-AR antibody (C-19) and 20 μl of protein A/G agarose. The quantitative real-time PCR was performed using soluble chromatin, immunoprecipitated DNAs, and the indicted primer pairs. The results of immunoprecipitated samples were corrected for the results of the corresponding soluble chromatin samples. All values represent at least three independent experiments. *Boxes*, Mean; *bars*, ± SD.

the domains of the nuclear receptors that interact with PGC-1α differed between nuclear receptors and between investigators (31, 54, 55). In our experiment, the TAD of AR interacted with PGC-1α. This result is supported by our finding that the interaction between AR and PGC-1α was not affected with or without androgen, suggesting that the LBD of AR was not involved in this interaction. Furthermore, our finding that deletion of the TAD of AR abolished the coactivator function of PGC-1α supported our finding that the TAD of AR is a region that interacts with the PGC-1α. This interaction up-regulated the transactivating ability of AR through the following mecha-

Downloaded from mend.endojournals.org at Kyushu Univ 00A Central Lib on February 16, 2010

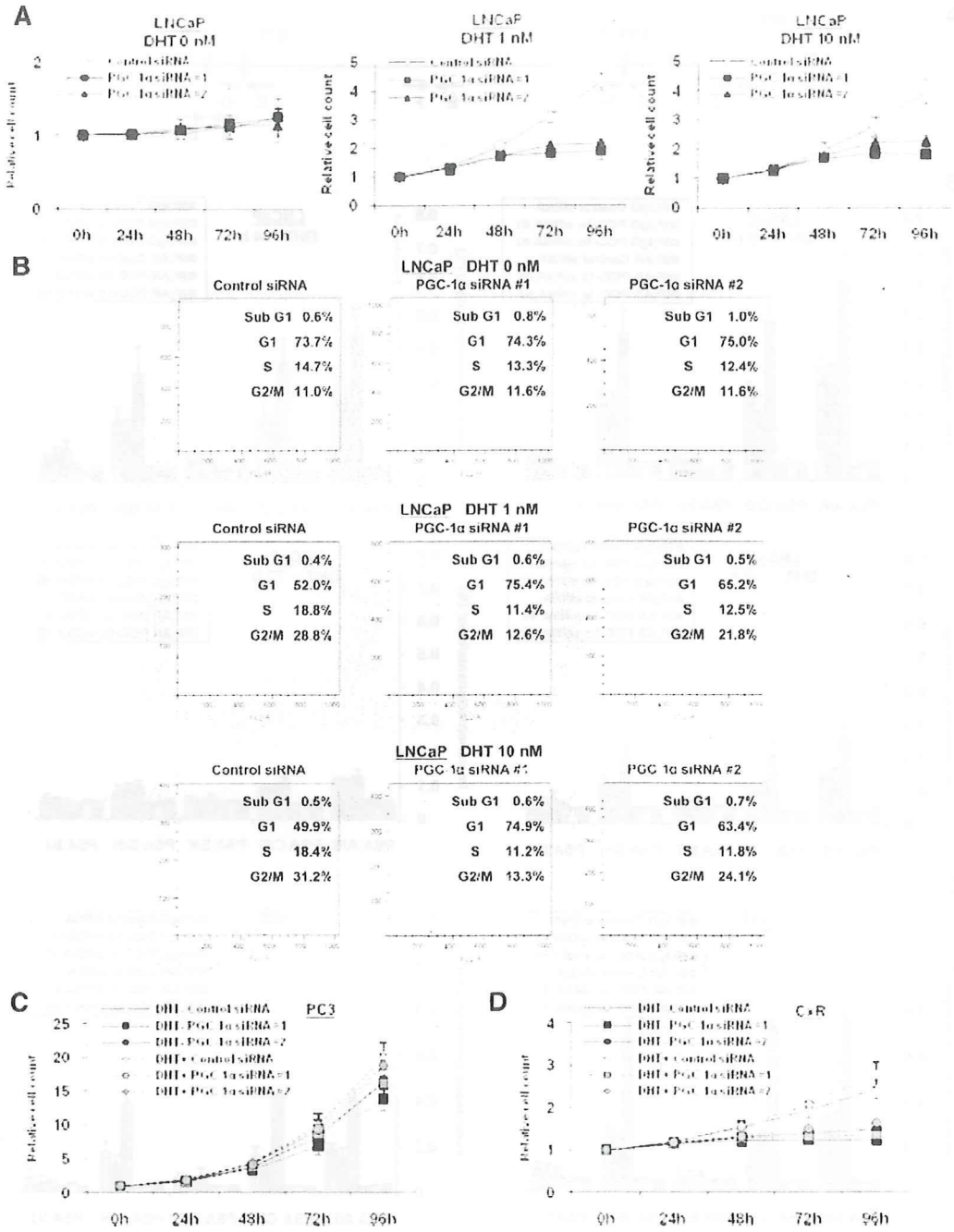

FIG. 7. Knock-down of PGC-1α suppresses cell proliferation in androgen-dependent and CRPC cells. A, LNCaP cells were transiently transfected with 50 nM of control siRNA, PGC-1α siRNA no. 1 or PGC-1α siRNA no. 2, and incubated in charcoal-stripped medium with 0, 1, or 10 nM of DHT. The cell numbers were counted at the indicated times. The results were normalized to cell numbers at hour 0. All values represent at least three independent experiments. *Boxes*, mean; *bars*, ± SD. B, LNCaP cells were transiently transfected with 50 nM of control siRNA, PGC-1α siRNA no. 1 or PGC-1α siRNA no. 2, and incubated in charcoal-stripped medium with 0, 1, or 10 nM of DHT. Seventy-two hours after transfection, the cells were stained with propidium iodide and analyzed by flow cytometry. The cell cycle fraction is shown in the *right upper* position of each graph. C and D, PC-3 (C) and CxR (D) cells were transiently transfected with 50 nM of control siRNA, PGC-1α siRNA no. 1 or PGC-1α siRNA no. 2, and incubated in charcoal-stripped medium with or without 10 nM of DHT. The cell proliferation assay was performed as described in A. *Boxes*, Mean; *bars*, ± SD.

nism. As indicated in Figs. 5 and 6, the interaction between PGC-1α and AR augmented the formation of a AR homodimer, leading to enhanced AR binding to the ARE and the expression of AR target genes.

Wirtenberger *et al.* (35) previously reported that the PGC-1α Thr612Met polymorphism was associated with familial breast cancer, high-risk familial breast cancer, and bilateral familial breast cancer risk in patients not carrying the BRCA 1/2 mutation (35). This finding suggests that PGC-1α function is involved in breast cancer carcinogenesis and progression by acting as a coactivator of ER. Therefore, we hypothesized that PGC-1α might

Downloaded from mend.endojournals.org at Kyushu Univ 00A Central Lib on February 16, 2010

also be involved in carcinogenesis and the progression of PCa, and investigated the effect of PGC-1α expression manipulation on androgen-dependent and CRPC cell growth. Our results showed that PGC-1α knock-down suppressed the growth of PCa cells. In particular, PGC-1α knock-down suppressed growth and cell-cycle arrest at the G_1 phase in AR-expressing PCa cells more effectively compared with PCa cells with no AR expression. This finding suggests that PGC-1α predominantly acts on PCa cells, at least in part, by interacting with and acting as a coactivator for AR. Although PC-3 cells expressing no AR mRNA and protein were also little affected by PGC-1α knock-down in the presence and absence of androgen, these effects may result from other functions of PGC-1α as other nuclear receptor coactivators, which was confirmed by the finding that cell growth suppression by PGC-1α knock-down was not affected by androgen depletion.

Also, PGC-1α and AR signaling are known to modulate metabolic activity. AR-null mice exhibit metabolic disease-like phenotype (56, 57). Similarly, PGC-1α knock-down reduced lipid metabolism, leading to storage of fat in adipocyte (58). Moreover, SRC-3, an AR coactivator was recently shown to induce PGC-1α acetylation and consequently inhibit its activity. Ablation of SRC-3 was subsequently found to improve insulin sensitivity (59). These findings support our results that PGC-1α interacts with AR and influences AR signaling. In addition, PGC-1α and AR signaling might be a useful therapeutic target for metabolic disease.

In conclusion, PGC-1α interacted with AR and activated the transcriptional function of AR. Also, PGC-1α knock-down delayed cell growth in AR expressing PCa cells. Furthermore, in castration-resistant LNCaP derivatives, CxR cells, PGC-1α knock-down suppressed cellular proliferation. Although PGC-1α expression needs to be investigated in PCa tissues compared with normal prostate glands, these findings indicate that the modulation of PGC-1α expression or function might be a useful strategy for developing novel therapeutics in PCa, which usually depends on androgens. Also, this strategy might be more useful for CRPC cells, which depends on AR signaling.

Materials and Methods

Cell culture

Human normal prostate epithelium RWPE-1 (keratinocyte serum-free medium), Human PCa DU145 (DMEM), PC-3 (Eagle's MEM), VCaP (DMEM), 22Rv1 (RPMI1640), and LNCaP cells (RPMI1640) were cultured in the indicated media. These media were purchased from Invitrogen (San Diego, CA) and contained 10% fetal bovine serum. LNCaP cells propagated between 10 and 30 times were used. Castration-resistant derivatives of LNCaP cells, LNCaP-CxR cells (referred to as CxR cells), were established and maintained as previously described (60). The cell lines were maintained in a 5% CO_2 atmosphere at 37°C.

Antibodies

Antibodies against AR (C-19, sc-815), AR (N-20, sc-7305), PSA (sc-7316), GFP (sc-8334), PGC-1α (sc-13067), and agarose-conjugated anti-GFP antibody (sc-8334 AC) were purchased from Santa Cruz Biotechnology (Santa Cruz, CA). Anti-Flag (M2) and anti-β-actin antibodies were purchased from Sigma (St. Louis, MO).

Plasmid construction

The AR-GFP plasmid expressing C-terminally GFP-tagged AR protein was kindly provided by T. Yanase (Fukuoka University, Fukuoka, Japan) (61). The pCMV-AR plasmid expressing wild-type AR, pCMV-ARmut877 plasmid expressing mutated AR (T877A), and MMTV-Luc were kindly provided by C. Chang (University of Rochester, Rochester, NY). The pGLP-SAp5.8 was kindly provided by A. Mizokami (Kanazawa University, Kanazawa, Japan) (62). To construct the AR-GFP 508-920 plasmid expressing GFP-tagged N-terminal deleted AR protein (from 508 to 920 aa), PCR was carried out with AR-GFP as a template using the following primer pairs: 5′-GCTAGCGGTACCCTGGCGGCATGGTGA-3′ and 5′-GGATCCACTGGGTGTGGAAATAGATGG-3′. The PCR product was cloned into the pEGFP vector (Clontech, Mountain View, CA). pCMV-AR 1-567 expressing C-terminal deleted AR protein (1-567 aa) was constructed by deletion of *Hin*dIII fragment from pCMV-AR plasmid. To obtain the full-length cDNA for AR, PCR was carried out with pCMV-AR as a template using the following primer pairs: 5′-ATGGAAGTG-CAGTTAGGGCTGG-3′ and 5′-TCACTGGGTGTG-GAAATAGATG-3′. The PCR product was cloned into the pGEM-T easy vector (Promega, Madison, WI). To construct pGEX-AR expressing GST-AR, a fragment of AR cDNA was ligated into the pGEX plasmid (GE Healthcare Bio-Science, Piscataway, NJ). The GST-AR deletion mutants (GST-AR 1-504, GST-AR 504-920, GST-AR 567-920, GST-AR 723-920, and GST-AR Δ715-844) were constructed from pGEX-AR full-length plasmid by deletion of the *Sph*I-*Acc*65I, *Acc*65I-*Hin*dIII, *Bam*HI-*Hin*dIII, *Sal*I-*Eco*RI, and *Bsr*GI fragments, respectively. GST-AR 504-721 was created from GST-AR 504-920 by deletion of the *Stu*I-*Not*I fragment.

The PGC-1α-Myc-Flag plasmid expressing the C-terminally Myc-Flag-tagged PGC-1α protein was purchased from OriGene (Rockville, MD). To obtain the full-length cDNA for PGC-1α, PCR was carried out with the PGC-1α-Myc-Flag plasmid as a template using the following primer pairs: 5′-GATGGCGTGG-GACATGTGCAACCA-3′ and 5′-TTACCTGCGCAAGCT-TCTCTGAGC-3′. The PCR product was cloned into the pGEM-T easy vector. To construct pGEX-PGC-1α expressing GST-PGC-1α, a fragment of PGC-1α cDNA was ligated into the pGEX plasmid. GST-PGC-1α deletion mutants (GST-PGC-1α 1-409, GST-PGC-1α 1-144, GST-PGC-1α 1-89, and GST-PGC-1α 294-798) were constructed from pGEX-PGC-1α full-length plasmid by deletion of the *Xba*I-*Not*I, *Afl*II-*Not*I, *Nhe*I-*Not*I, and *Bam*HI-*Stu*I fragments, respectively. To construct GST-PGC-1α 1-186, N-terminal *Eco*RI fragment of cDNA for PGC-1α was ligated into the pGEX plasmid.

Downloaded from mend.endojournals.org at Kyushu Univ 00A Central Lib on February 16, 2010

Western blot analysis

Whole-cell lysates and nuclear extracts were prepared as previously described (60, 63–66). The protein concentration of the extracts was quantified using a Protein Assay kit based on the Bradford method (Bio-Rad, Hercules, CA). The indicated amounts of whole-cell lysates and nuclear extracts were separated by 4–20% SDS-PAGE and transferred to polyvinylidene difluoride microporous membranes (GE Healthcare Bio-Science) using a semidry blotter. The blotted membranes were incubated for 1 h at room temperature with the primary antibodies described above. The membranes were then incubated for 40 min at room temperature with a peroxidase-conjugated secondary antibody. The bound antibody was visualized using an ECL kit (GE Healthcare Bio-Science), and the membranes were exposed to Kodak X-OMAT film.

Expression of GST-fusion proteins in *Escherichia coli*

GST-fusion proteins in *E. coli* were prepared as previously described (64–66). To express GST-fusion proteins, bacteria transformed with expression plasmids were incubated with 1 mM isopropyl-β-D-thiogalactopyranoside (Nacalai tesque, Kyoto, Japan) for 2 h at room temperature and collected by centrifugation. The cells were sonicated (TAITEC sonicator, Tokyo, Japan) in buffer X containing 50 mM Tris-HCl (pH 8.0), 1 mM EDTA, 120 mM NaCl, 0.5% (vol/vol) Nonidet P-40 (NP-40), 10% (vol/vol) glycerol, 1 mM phenylmethylsulfonyl fluoride, and 1 mM dithiothreitol, and the cell lysates were collected after centrifugation at 21,000 *g* for 10 min at 4°C.

GST pull-down assay

The GST pull-down assay was performed as previously described (64–66). GST-AR, GST-PGC-1α, or their deletion mutants immobilized on glutathione-sepharose 4B (GE Healthcare Bio-Science) were incubated with soluble cell extracts for 2 h at 4 C in buffer X. The bound samples were washed three times with buffer X and subjected to Western blot analysis with the indicated antibodies.

Coimmunoprecipitation assay

The transient transfection and immunoprecipitation assays were performed as previously described (64–66). Briefly, 1×10^5 LNCaP and PC-3 cells were transfected with the indicated amounts of each of the indicated expression plasmids using Lipofectamine 2000 (Invitrogen) according to the manufacturer's instructions and seeded into six-well plates. After incubation at 37°C for 48 h with the indicated fresh medium, the cells were lysed in buffer X. The lysates were centrifuged at 21,000 × *g* for 10 min at 4°C, and the supernatants (300 μg) were incubated for 2 h at 4°C with agarose-conjugated anti-GFP antibody. The immunoprecipitated samples were washed three times with buffer X, and the preimmunoprecipitated samples (30 μg) were subjected to Western blot analysis with the indicated antibodies. Signal intensities of preimmunoprecipitated and coimmunoprecipitated AR protein were quantified using the NIH Imaging program (NIH, Bethesda, MD). The intensities of coimmunoprecipitated AR protein were corrected for the corresponding intensities of preimmunoprecipitated AR protein. The results are representative of at least three independent experiments.

For immunoprecipitation assays without transient transfection, 70–80% confluent LNCaP cells were cultured in 100-mm tissue-culture plates with the indicated medium for 48 h and lysed with buffer X. The lysates were centrifuged at 21,000 × *g* for 10 min at 4 C, and the supernatants (500 μg) were incubated overnight at 4 C with 2.0 μg of rabbit IgG or anti-AR antibody. The immunoprecipitated samples were washed three times with buffer X, and the preimmunoprecipitated samples (50 μg) were subjected to Western blot analysis with the indicated antibodies.

Knock-down analysis using siRNAs

Knock-down analysis using siRNA was performed as previously described (60, 63–66). The following double-stranded RNA 25-base-pair oligonucleotides were commercially generated (Invitrogen): 5′-AAUCUGUGGAAGAACAAAUCUGCCC-3′ (sense) and 5′-GGGCAGAUUUGUUCUUCCACAGAUU-3′ (antisense) for PGC-1α siRNA no. 1; 5′-UAUUCUUCCCUCUUCAGCCUCUCGU-3′ (sense) and 5′-ACGAGAGGCUGAAGAGGGAAGAAUA-3′ (antisense) for PGC-1α siRNA no. 2. LNCaP, CxR and PC-3 cells were transfected with siRNA using Lipofectamine 2000 according to the manufacturer's instructions.

RNA isolation and RT-PCR

Total RNA was prepared from cultured cells using RNeasy mini kits (QIAGEN, Valencia, CA). First-strand cDNA was synthesized from 1.0 μg of total RNA using a Transcriptor First-Strand cDNA Synthesis Kit (Roche Applied Science, Indianapolis, IN) according to the manufacturer's instructions.

Quantitative real-time PCR

The synthesized cDNA was diluted 1:2, and 2.0 μl of the diluted mixture was used. Quantitative real-time PCR with TaqMan Gene Expression Assay (Applied Biosystems, Foster City, CA) and TaqMan Gene Expression Master Mix (Applied Biosystems) was performed using ABI 7900HT (Applied Biosystems). The expression level of AR and PSA mRNA was corrected for the corresponding glyceraldehyde 3-phosphate dehydrogenase (GAPDH) mRNA expression level. The results are representative of at least three independent experiments.

Luciferase reporter assay

The luciferase reporter assay was performed as previously described (60). Briefly, LNCaP and PC-3 cells (1.5×10^5) were cotransfected with the indicated amounts of reporter plasmids, 0.05 μg of pRL-TK as an internal control and the indicated amounts of expression plasmids or siRNA using Lipofectamine 2000 according to the manufacturer's instructions and seeded into 12-well plates. After incubation for 48 h, luciferase activity was detected using a Dual-Luciferase Reporter Assay System (Promega). Light intensity was measured using a plate reader (ARVO™ MX; Perkin Elmer Inc., Waltham, MA). *Firefly* luciferase activity was corrected for the corresponding *Renilla* luciferase activity. The results are representative of at least three independent experiments.

Chromatin immunoprecipitation assay

Chromatin immunoprecipitation assay was performed as previously described (60, 63, 65). Briefly, LNCaP and CxR cells were transfected with control siRNA, PGC-1α siRNA no. 1 or PGC-1α siRNA no. 2, seeded into six-well plates, and incubated for 72 h. Soluble chromatin from 1×10^6 cells was incubated overnight at 4°C with 2.0 μg of antirabbit IgG or anti-AR an-

Downloaded from mend.endojournals.org at Kyushu Univ 00A Central Lib on February 16, 2010

tibody and 20 μl of protein A/G agarose. Purified DNA was dissolved in 20 μl of dH_2O, and 1 μl of the diluted mixture was used for PCR analysis with the following primer pairs: 5′-TCTGCCTTTGTCCCCTAGAT-3′ (forward) and 5′-AACCTTCATTCCCCAGGACT-3′ (reverse) for PSA A/B (−250 bp to −39 bp); 5′-AGGGATCAGGGAGTCTCACA-3′ (forward) and 5′-GCTAGCACTTGCTGTTCTGC-3′ (reverse) for PSA C/D (−406 bp to −164 bp); 5′-CTGTGCTTGGAGTTTACCTGA-3′ (forward) and 5′-GCAGAGGTTGCAGTGAGCC-3′ (reverse) for PSA E/F (−1997 bp to −1846 bp); 5′-CCTCCCAGGTTCAAGTGATT-3′ (forward) and 5′-GCCTGTAATCCCAGCACTTT-3′ (reverse) for PSA G/H (−4170 bp to −3978 bp); 5′-GATGGTGTTTCACCGTGTTG-3′ (forward) and 5′-AGAGTGCAGTGAGCCGAGAT-3′ (reverse) for PSA I/J (−7694 bp to −7484 bp). These primer pairs were described previously (39). The PCR products were separated by electrophoresis on 2% agarose gels and stained with ethidium bromide. The quantitative real-time PCR assay with 1 μl of the diluted DNA, the above primer pairs and SYBR Premix Ex Taq II (Takara Bio, Shiga, Japan) was performed using ABI 7900HT. The results are representative of at least three independent experiments.

Cell proliferation assay

The cell proliferation assay was performed as previously described (60, 63, 64, 66). Briefly, 2.0×10^4 LNCaP, CxR and PC-3 cells were transfected with control siRNA, PGC-1α siRNA no. 1 or PGC-1α siRNA no. 2, as described above and seeded in 12-well plates, and incubated in the indicated medium. Twelve hours after transfection was set as hour 0. The cells were harvested with trypsin and counted daily using a cell counter (Beckman Coulter, Fullerton, CA). The results were normalized to cell counts at h 0, and are representative of at least three independent experiments.

Flow cytometry analysis

The flow cytometry analysis was performed as previously described (60, 63). Briefly, 2.5×10^5 LNCaP cells were transfected with control siRNA, PGC-1α siRNA no. 1 or PGC-1α siRNA no. 2, seeded in six-well plates, and incubated in the indicated medium for 72 h. The cells were harvested, washed twice with ice-cold PBS with 0.1% BSA, and resuspended in 70% ethanol. After washing twice with ice-cold PBS, the cells were resuspended in PBS with 0.1% BSA, incubated with RNase (Roche Molecular Biochemicals, Basel, Switzerland), and stained with propidium iodide (Sigma). Cells were analyzed using a FACS Calibur (BD Biosciences, San Jose, CA).

Acknowledgments

We thank Dr. Toshihiko Yanase, Dr. Chawnshang Chang, and Dr. Atsushi Mizokami for providing the plasmids; Dr. Dongchon Kang (Kyushu University, Fukuoka, Japan) for helping with quantitative real-time PCR and flow cytometry; and Noriko Hakoda, Hitomi Matoba, and Seiko Kamori for their technical assistance.

Address all correspondence and requests for reprints to: Akira Yokomizo M.D., Ph.D., Department of Urology, Graduate School of Medical Sciences, Kyushu University, 3-1-1 Maidashi, Higashi-ku, Fukuoka 812-8252, Japan. E-mail: yokoa@uro.med.kyushu-u.ac.jp.

This work was supported by Health Sciences Research Grants for Clinical Research for Evidenced Based Medicine and Grant-in-Aid for Cancer Research 016 from the Ministry of Health, Labor, and Welfare, Japan; and by a Young Researcher Promotion grant from the Japanese Urological Association, Japan.

Disclosure Summary: The authors have nothing to disclose.

References

1. Grönberg H 2003 Prostate cancer epidemiology. Lancet 361:859–864
2. Hsing AW, Devesa SS 2001 Trends and patterns of prostate cancer: what do they suggest? Epidemiol Rev 23:3–13
3. Feldman BJ, Feldman D 2001 The development of androgen-independent prostate cancer. Nat Rev Cancer 1:34–45
4. Han M, Partin AW, Piantadosi S, Epstein JI, Walsh PC 2001 Era specific biochemical recurrence-free survival following radical prostatectomy for clinically localized prostate cancer. J Urol 186:416–419
5. Isaacs W, De Marzo A, Nelson WG 2002 Focus on prostate cancer. Cancer Cell 2:113–116
6. Debes JD, Tindall DJ 2002 The role of androgens and the androgen receptor in prostate cancer. Cancer Lett 187:1–7
7. Scher HI, Sawyers CL 2005 Biology of progressive, castration-resistant prostate cancer: directed therapies targeting the androgen-receptor signaling axis. J Clin Oncol 23:8253–8261
8. Gregory CW, Hamil KG, Kim D, Hall SH, Pretlow TG, Mohler JL, French FS 1998 Androgen receptor expression in androgen-independent prostate cancer is associated with increased expression of androgen-regulated genes. Cancer Res 58:5718–5724
9. Chen CD, Welsbie DS, Tran C, Baek SH, Chen R, Vessella R, Rosenfeld MG, Sawyers CL 2004 Molecular determinants of resistance to antiandrogen therapy. Nat Med 10:33–39
10. Zegarra-Moro OL, Schmidt LJ, Huang H, Tindall DJ 2002 Disruption of androgen function inhibits proliferation of androgen-refractory prostate cancer cells. Cancer Res 62:1008–1013
11. Linja MJ, Savinainen KJ, Saramäki OR, Tammela TL, Vessella RL, Visakorpi T 2001 Amplification and overexpression of androgen receptor gene in hormone-refractory prostate cancer. Cancer Res 61:3550–3555
12. Taplin ME, Rajeshkumar B, Halabi S, Werner CP, Woda BA, Picus J, Stadler W, Hayes DF, Kantoff PW, Vogelzang NJ, Small EJ 2003 Androgen receptor mutations in androgen-independent prostate cancer: Cancer and Leukemia Group B Study 9663. J Clin Oncol 21:2673–2678
13. Culig Z, Hobisch A, Cronauer MV, Radmayr C, Trapman J, Hittmair A, Bartsch G, Klocker H 1994 Androgen receptor activation in prostate tumor cell lines by insulin-like growth factor-I, keratinocyte growth factor, and epidermal growth factor. Cancer Res 54:5474–5478
14. Craft N, Shostak Y, Carey M, Sawyers CL 1999 A mechanism for hormone-independent prostate cancer through modulation of androgen receptor signaling by the HER-2/*neu* tyrosine kinase. Nat Med 5:280–285
15. Hobisch A, Eder IE, Putz T, Horninger W, Bartsch G, Klocker H, Culig Z 1998 Interleukin-6 regulates prostate-specific protein expression in prostate carcinoma cells by activation of the androgen receptor. Cancer Res 58:4640–4645
16. Zoubeidi A, Zardan A, Beraldi E, Fazli L, Sowery R, Rennie P, Nelson C, Gleave M 2007 Cooperative interaction between androgen receptor (AR) and heat-shock protein 27 facilitate AR transcriptional activity. Cancer Res 67:10455–10465
17. Park SY, Yu X, Ip C, Mohler JL, Bogner PN, Park YM 2007 Peroxiredoxin 1 interacts with androgen receptor and enhances its transactivation. Cancer Res 67:9294–9303

Downloaded from mend.endojournals.org at Kyushu Univ 00A Central Lib on February 16, 2010

18. Gaughan L, Logan IR, Cook S, Neal DE, Robson CN 2002 Tip60 and histone deacetylase 1 regulate androgen receptor activity through changes to the acetylation status of the receptor. J Biol Chem 277:25904–25913
19. Miyamoto H, Rahman M, Takatera H, Kang HY, Yeh S, Chang HC, Nishimura K, Fujimoto N, Chang C 2002 A dominant-negative mutant of androgen receptor coregulator ARA-54 inhibits androgen receptor-mediated prostate cancer growth. J Biol Chem 277:4609–4617
20. Fujimoto N, Yeh S, Kang HY, Inui S, Chang HC, Mizokami A, Chang C 1999 Cloning and characterization of androgen receptor coactivator, ARA55, in human prostate. J Biol Chem 274:8316–8321
21. Rahman MM, Miyamoto H, Taketera H, Yeh S, Altuwaijri S, Chang C 2003 Reducing the agonist activity of antiandrogens by a dominant-negative androgen receptor coregulator ARA70 in prostate cancer cells. J Biol Chem 278:19619–19626
22. Hong H, Kohli K, Garabedian MJ, Stallcup MR 1997 GRIP1, a transcriptional coactivator for the AF-2 transactivation domain of steroid, thyroid, retinoid, and vitamin D receptors. Mol Cell Biol 17:2735–2744
23. Boonyaratanakornkit V, Melvin V, Prendergast P, Altmann M, Ronfani L, Bianchi ME, Taraseviciene L, Nordeen SK, Allegretto EA, Edwards DP 1998 High-mobility group chromatin proteins 1 and 2 functionally interact with steroid hormone receptors to enhance their DNA binding in vitro and transcriptional activity in mammalian cells. Mol Cell Biol 18:4471–4487
24. Gross M, Liu B, Tan J, French FS, Carey M, Shuai K 2001 Distinct effects of PIAS proteins on androgen-mediated gene activation in prostate cancer cells. Oncogene 20:3880–3887
25. Bevan CL, Hoare S, Claessens F, Heery DM, Parker MG 1999 The AF1 and AF2 domains of the androgen receptor interact with distinct regions of SRC1. Mol Cell Biol 19:8383–8392
26. Puigserver P, Wu Z, Park CW, Graves R, Wright M, Spiegelman BM 1998 A cold-inducible coactivator of nuclear receptors linked to adaptive thermogenesis. Cell 92:829–839
27. Knutti D, Kaul A, Kralli A 2000 A tissue-specific coactivator of steroid receptors, identified in a functional genetic screen. Mol Cell Biol 20:2411–2422
28. Wu Z, Puigserver P, Andersson U, Zhang C, Adelmant G, Mootha V, Troy A, Cinti S, Lowell B, Scarpulla RC, Spiegelman BM 1999 Mechanisms controlling mitochondrial biogenesis and respiration through the thermogenic coactivator PGC-1. Cell 98:115–124
29. Kressler D, Schreiber SN, Knutti D, Kralli A 2002 The PGC-1-related protein PERC is a selective coactivator of estrogen receptor α. J Biol Chem 277:13918–13925
30. Tcherepanova I, Puigserver P, Norris JD, Spiegelman BM, McDonnell DP 2000 Modulation of estrogen receptor-α transcriptional activity by the coactivator PGC-1. J Biol Chem 275:16302–16308
31. Bourdoncle A, Labesse G, Margueron R, Castet A, Cavaillès V, Royer CA 2005 The nuclear receptor coactivator PGC-1α exhibits modes of interaction with the estrogen receptor distinct from those of SRC-1. J Mol Biol 347:921–934
32. Castillo G, Brun RP, Rosenfield JK, Hauser S, Park CW, Troy AE, Wright ME, Spiegelman BM 1999 An adipogenic cofactor bound by the differentiation domain of PPARγ. EMBO J 18:3676–3687
33. Anderson E 2002 The role of oestrogen and progesterone receptors in human mammary development and tumorigenesis. Breast Cancer Res 4:197–201
34. Fishman J, Osborne MP, Telang NT 1995 The role of estrogen in mammary carcinogenesis. Ann NY Acad Sci 768:91–100
35. Wirtenberger M, Tchatchou S, Hemminki K, Schmutzhard J, Sutter C, Schmutzler RK, Meindl A, Wappenschmidt B, Kiechle M, Arnold N, Weber BH, Niederacher D, Bartram CR, Burwinkel B 2006 Association of genetic variants in the estrogen receptor coactivators PPARGC1A, PPARGC1B and EP300 with familial breast cancer. Carcinogenesis 27:2201–2208
36. Shenk JL, Fisher CJ, Chen SY, Zhou XF, Tillman K, Shemshedini L 2001 p53 Represses androgen-induced transactivation of prostate-specific antigen by disrupting hAR amino- to carboxyl-terminal interaction. J Biol Chem 42:38472–38479
37. Li J, Fu J, Toumazou C, Yoon HG, Wong J 2006 A role of the amino-terminal (N) and carboxyl-terminal (C) interaction in binding of androgen receptor to chromatin. Mol Endocrinol 20:776–785
38. Need EF, Scher HI, Peters AA, Moore NL, Cheong A, Ryan CJ, Wittert GA, Marshall VR, Tilley WD, Buchanan G 2009 A novel androgen receptor amino terminal region reveals two classes of amino/carboxyl interaction-deficient variants with divergent capacity to activate responsive sites in chromatin. Endocrinology 150: 2674–2682
39. Shang Y, Myers M, Brown M 2002 Formation of the androgen receptor transcription complex. Mol Cell 9:601–610
40. Tyagi RK, Lavrovsky Y, Ahn SC, Song CS, Chatterjee B, Roy AK 2000 Dynamics of intracellular movement and nucleocytoplasmic recycling of the ligand-activated androgen receptor in living cells. Mol Endocrinol 14:1162–1174
41. Debes JD, Sebo TJ, Lohse CM, Murphy LM, Haugen DA, Tindall DJ 2003 p300 In prostate cancer proliferation and progression. Cancer Res 63:7638–7640
42. Powell SM, Christiaens V, Voulgaraki D, Waxman J, Claessens F, Bevan CL 2004 Mechanisms of androgen receptor signaling via steroid receptor coactivator-1 in prostate. Endocr Relat Cancer 11:117–130
43. Abate-Shen C, Shen MM 2000 Molecular genetics of prostate cancer. Genes Dev 14:2410–2434
44. McKenna NJ, Lanz RB, O'Malley BW 1999 Nuclear receptor coregulators: cellular and molecular biology. Endocr Rev 29:321–344
45. McKenna NJ, O'Malley BW 2002 Combined control of gene expression by nuclear receptors and coregulators. Cell 108:465–474
46. Linja MJ, Porkka KP, Kang Z, Savinainen KJ, Jänne OA, Tammela TL, Vessella RL, Palvimo JJ, Visakorpi T 2004 Expression of androgen receptor coregulators in prostate cancer. Clin Cancer Res 10:1032–1040
47. Oñate SA, Tsai SY, Tsai MJ, O'Malley BW 1995 Sequence and characterization of a coactivator for the steroid hormone receptor superfamily. Science 270:1354–1357
48. Zhou HJ, Yan J, Luo W, Ayala G, Lin SH, Erdem H, Ittmann M, Tsai SY, Tsai MJ 2005 SRC-3 is required for prostate cancer cell proliferation and survival. Cancer Res 65:7976–7983
49. Shi XB, Xue L, Zou JX, Gandour-Edwards R, Chen H, deVere White RW 2008 Prolonged androgen receptor loading onto chromatin and the efficient recruitment of p160 coactivators contribute to androgen-independent growth of prostate cancer cells. Prostate 68:1816–1826
50. Heemers HV, Sebo TJ, Debes JD, Regan KM, Raclaw KA, Murphy LM, Hobisch A, Culig Z, Tindall DJ 2007 Androgen deprivation increases p300 expression in prostate cancer cells. Cancer Res 67: 3422–3430
51. Heery DM, Kalkhoven E, Hoare S, Parker MG 1997 A signature motif in transcriptional co-activators mediates binding to nuclear receptors. Nature 387:733–736
52. Voegel JJ, Heine MJ, Tini M, Vivat V, Chambon P, Gronemeyer H 1998 The coactivator TIF2 contains three nuclear receptor-binding motifs and mediates transactivation through CBP binding-dependent and -independent pathways. EMBO J 17:507–519
53. McInerney EM, Weis KE, Sun J, Mosselman S, Katzenellenbogen BS 1998 Transcription activation by the human estrogen receptor subtype β (ERβ) studied with ERβ and ERα receptor chimeras. Endocrinology 139:4513–4522
54. Greschik H, Althage M, Flaig R, Sato Y, Chavant V, Peluso-Iltis C, Choulier L, Cronet P, Rochel N, Schüle R, Strömstedt PE, Moras D 2008 Communication between the ERRα homodimer interface and the PGC-1α binding surface via the helix 8–9 loop. J Biol Chem 283:20220–20230
55. Delerive P, Wu Y, Burris TP, Chin WW, Suen CS 2002 PGC-1

Downloaded from mend.endojournals.org at Kyushu Univ 00A Central Lib on February 16, 2010

functions as a transcriptional coactivator for the retinoid X receptors. J Biol Chem 277:3913–3917
56. Sato T, Otaka M, Odashima M, Kato S, Jin M, Konishi N, Matsuhashi T, Watanabe S 2006 Specific type IV phosphodiesterase inhibitor ameliorates cerulein-induced pancreatitis in rats. Biochem Biophys Res Commun 346:339–344
57. Yanase T, Fan W, Kyoya K, Min L, Takayanagi R, Kato S, Nawata H 2008 Androgens and metabolic syndrome: lessons from androgen receptor knock out (ARKO) mice. J Steroid Biochem Mol Biol 109:254–257
58. Sanyal S, Matthews J, Bouton D, Kim HJ, Choi HS, Treuter E, Gustafsson JA 2004 Deoxyribonucleic acid response element-dependent regulation of transcription by orphan nuclear receptor estrogen receptor-related receptor γ. Mol Endocrinol 18:312–325
59. Coste A, Louet JF, Lagouge M, Lerin C, Antal MC, Meziane H, Schoonjans K, Puigserver P, O'Malley BW, Auwerx J 2008 The genetic ablation of SRC-3 protects against obesity and improves insulin sensitivity by reducing the acetylation of PGC-1α. Proc Natl Acad Sci USA 105:17187–17192
60. Shiota M, Yokomizo A, Tada Y, Inokuchi J, Kashiwagi E, Masubuchi D, Eto M, Uchiumi T, Naito S, Castration resistance of prostate cancer cells caused by castration-induced oxidative stress through Twist1 and androgen receptor overexpression. Oncogene 10.1038/onc.2009.322
61. Tomura A, Goto K, Morinaga H, Nomura M, Okabe T, Yanase T, Takayanagi R, Nawata H 2001 The subnuclear three-dimensional image analysis of androgen receptor fused to green fluorescence protein. J Biol Chem 276:28395–28401
62. Mizokami A, Gotoh A, Yamada H, Koller ET, Matsumoto T 2000 Tumor necrosis factor-α represses androgen sensitivity in the LNCaP prostate cancer cell line. J Urol 164:800–805
63. Shiota M, Izumi H, Onitsuka T, Miyamoto N, Kashiwagi E, Kidani A, Yokomizo A, Naito S, Kohno K 2008 Twist promotes tumor cell growth through YB-1 expression. Cancer Res 68:98–105
64. Shiota M, Izumi H, Onitsuka T, Miyamoto N, Kashiwagi E, Kidani A, Hirano G, Takahashi M, Naito S, Kohno K 2008 Twist and p53 reciprocally regulate target genes via direct interaction. Oncogene 27:5543–5553
65. Shiota M, Izumi H, Miyamoto N, Onitsuka T, Kashiwagi E, Kidani A, Hirano G, Takahashi M, Ono M, Kuwano M, Naito S, Sasaguri Y, Kohno K 2008 Ets regulates peroxiredoxin1 and 5 expressions through their interaction with the high mobility group protein B1. Cancer Sci 99:1950–1959
66. Shiota M, Izumi H, Tanimoto A, Takahashi M, Miyamoto N, Kashiwagi E, Kidani A, Hirano G, Masubuchi D, Fukunaka Y, Yasuniwa Y, Naito S, Nishizawa S, Sasaguri Y, Kohno K 2009 Programmed cell death protein 4 down-regulates Y-box binding protein-1 expression via a direct interaction with Twist1 to suppress cancer cell growth. Cancer Res 69:3148–3156

Downloaded from mend.endojournals.org at Kyushu Univ 00A Central Lib on February 16, 2010

Int. J. Cancer: **125**, 2836–2843 (2009)
© 2009 UICC

The novel tumor-suppressor Mel-18 in prostate cancer: Its functional polymorphism, expression and clinical significance

Wei Wang[1,2], Takeshi Yuasa[2,3]*, Norihiko Tsuchiya[2], Zhiyong Ma[2], Shinya Maita[2], Shintaro Narita[2], Teruaki Kumazawa[2], Takamitsu Inoue[2], Hiroshi Tsuruta[2], Yohei Horikawa[2], Mitsuru Saito[2], Weilie Hu[1], Osamu Ogawa[4] and Tomonori Habuchi[2]

[1]*Department of Urology, Guangzhou Liuhuaqiao Hospital Guangzhou General Hospital of Guangzhou Military Command, Guangzhou, Guangdong province, China*

[2]*Department of Medical Oncology and Genitourinary Oncology, Cancer Institute Hospital, Japanese Foundation for Cancer Research, 3-10-6 Ariake, Koto-ward, Tokyo, 135-8550, Japan*

[3]*Department of Medical Oncology and Genitourinary Oncology, Cancer Institute Hospital of Japanese Foundation for Cancer Research, 3-10-6 Ariake, Koto-ward, Tokyo, 135-8550, Japan*

[4]*Department of Urology, Kyoto University Graduate School of Medicine, 54 Shogoin Kawahara, Sakyo-ku, Kyoto, 606-8507, Japan*

Mel-18 is a member of the polycomb group (PcG) proteins, which are chromatin regulatory factors and play important roles in development and oncogenesis. This study was designed to investigate the clinical and prognostic significance of Mel-18 in patients with prostate cancer. A total of 539 native Japanese subjects consisting of 393 prostate cancer patients and 146 controls were enrolled in this study. *Mel-18* genotyping was analyzed using a PCR-RFLP method and an automated sequencer using the GENESCAN software. Immunohistochemistry revealed that Mel-18 expression was diminished in high grade and high stage prostate cancers. Moreover, patients with positive Mel-18 expression had significantly longer PSA recurrence-free survival than patients negative for Mel-18 expression ($p = 0.038$). A Mel-18 *1805A/G* SNP was located in the 3' untranslated region and was predicted to alter the secondary structure of the mRNA. *Mel-18* mRNA expression of the 1805*A* allele was clearly higher than expression of the 1805*G* allele by allele specific quantitative RT-PCR. In multivariate analysis, a homozygous *G* allele genotype and negative Mel-18 expression were independent risk factors predicting high PSA recurrence after radical prostatectomy, with HRs of 2.757 ($p = 0.022$) and 2.271 ($p = 0.045$), respectively. Moreover, the *G* allele was also an independent predictor of poor cancer-specific survival with an HR of 4.658 ($p = 0.019$) for patients with stage D2 prostate cancer. This is the first study to provide important evidence demonstrating that Mel-18 is a tumor suppressor and possible therapeutic target, as well as a diagnostic marker for poor prognosis in prostate cancer patients.
© *2009 UICC*

Key words: Mel-18; SNP; polycomb group protein; prostate cancer; PCGF2

Polycomb group (PcG) proteins are chromatin regulatory factors that play important roles in development and oncogenesis.[1] Among the PcG family, Bmi-1 is the best characterized protein, and is defined as an oncogene product expressed not only in hematological malignancies but also in various solid tumors.[2–4] Overexpression of Bmi-1-drives an oncogenic pathway demonstrated to lead to a marked propensity for metastatic dissemination as well as a high probability of a poor prognosis in a wide range of cancers including prostate cancer.[5,6] *Mel-18*, which is officially called as PcG RING finger protein 2 (PCGF2), is a member of the PcG gene family whose protein product is structurally highly similar to Bmi-1.[7] Although *Bmi-1* is known to play a role in oncogenesis as a c-*myc* cooperating oncogene, some investigators have reported that *Mel-18* acts as a tumor suppressor *via* transcriptional repression of Bmi-1 and c-Myc.[8–11] *Mel-18* is located at chromosome 17q12, a region associated with prostate cancer risk by previous studies.[12,13]

We hypothesized that Mel-18 may function as tumor suppressor and its expression may alter the clinical behavior of prostate cancer patients. To date, there has been no report investigating the association between Mel-18 and clinicopathological variables of prostate cancer. This study was designed to test our hypothesis and determine the clinical significance of Mel-18 in patients with prostate cancer.

Material and methods

Subjects

A total of 539 native Japanese subjects consisting of 393 prostate cancer patients and 146 controls were enrolled in our study. Control subjects were selected randomly from native Japanese men undergoing a regular medical check-up at the community hospitals in the Akita prefecture. This study was approved by the ethics committee of the Akita University School of Medicine. All of the patients with prostate cancer were treated at these hospitals from April 1997 to December 2003. Written informed consent was obtained from all patients for the use of their DNA and clinical information. The pathological grade and clinical stage of the prostate cancers were determined according to the Tumor-Node-Metastatic system, the Gleason histological grading system and the modified Whitmore-Jewett system, as described previously.[14–17]

Seven renal cancers and surrounding non-cancerous tissues, 8 bladder cancers and surrounding non-cancerous tissues, and 12 non-cancerous prostatic tissues were obtained immediately after resection.

Cell lines were obtained from the American Tissue Type Culture collection (ATCC, Manassas, VA). Two prostate cancer lines, DU145 and PC3, 6 kidney cancer lines, RPMI/SE, CAKI-1, NC65, OSRC2, CCFRC1 and ACHN and 5 bladder cancer lines, 253J, UM-UC-3, TCCSUP, 5637 and KU7, were used for a Mel-18 reverse transcription-polymerase chain reaction (RT-PCR) study.

Immunohistochemical staining

Mel-18 goat polyclonal antibody (Santa Cruz Biotechnology, Inc., Santa Cruz, CA) at a dilution of 1:400 was used as primary antibody. Immunohistochemical staining was performed using a standard avidin-biotin-peroxidase complex method (Histofine, Nichirei, Tokyo, Japan), as described previously.[18]

Additional Supporting Information may be found in the online version of this article.

Grant sponsor: The Takeda Science Foundation, the Kobayashi Institute for Innovative Cancer Chemotherapy, the Shimadzu Science Foundation, the Sagawa Foundation for Promotion of Cancer Research, the Japan-China Sasakawa Medical Fellowship, Grants-in-Aid for Scientific Research from the Ministry of Education, Culture, Sports, Science and Technology, Japan, and the GCOE program of the Ministry of Education, Culture, Sports, Science and Technology, Japan.

***Correspondence to:** Department of Medical Oncology and Genitourinary Oncology, Cancer Institute Hospital of Japanese Foundation for Cancer Research, 3-10-6 Ariake, Koto-ward, Tokyo, 135-8550, Japan. Fax: 81-3-3570-0343. E-mail: takeshi.yuasa@jfcr.or.jp

Received 15 April 2009; Accepted after revision 12 June 2009

DOI 10.1002/ijc.24721

Published online 7 July 2009 in Wiley InterScience (www.interscience.wiley.com).

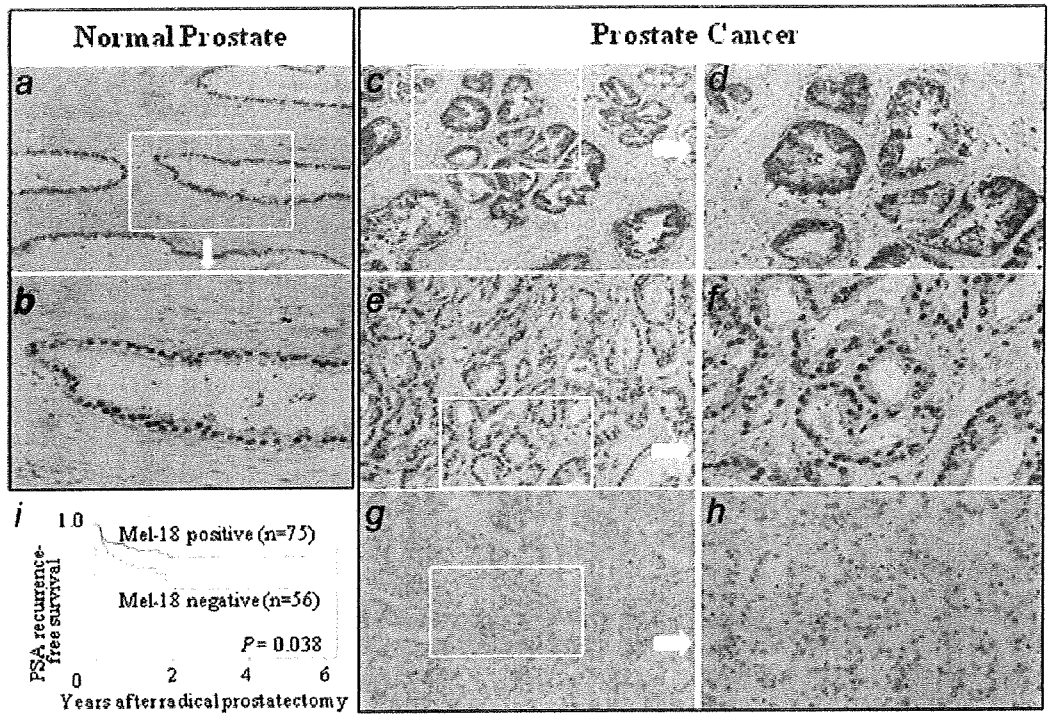

FIGURE 1 – Mel-18 expression and clinical significance. Representative Mel-18 expression in normal (*a,b*) and prostate cancer (*c–h*) tissues. Strong nuclear staining is observed in the non-malignant prostate (*a,b*) whereas various expression patterns including strong (*c,d*), moderate (*e, f*), and weak (*g,h*) expressions, were exhibited by prostate cancer tissues. PSA recurrence-free survival of patients who underwent radical prostatectomy stratified by Mel-18 expression status (*i*).

Immunohistochemical evaluation

Staining results were assessed independently by two investigators (W.W. and M.Z.) in a semi-quantitative fashion at a magnification of 200× (Fig. 1). The staining intensity scores were: 1 (no staining at all), 2 (weak), 3 (medium), and 4 (strong). The staining extent was scored according to the percentage of positive cells: 1 (0% to 5%), 2 (6% to 35%), 3 (36% to 70%), and 4 (71% to 100%). A final score was then calculated by multiplying the above two scores. When the final score was ≥4, the tumor was considered positive for Mel-18 expression; otherwise, the tumor was considered negative. This categorization is fundamentally similar to that used in a previous immunohistochemical study.[10]

Mel-18 genotyping analysis

Mel-18 genotyping was analyzed by a PCR- RFLP method. A 110 bp DNA fragment spanning the *1805A/G* single nucleotide polymorphism (SNP, rs708692) in the *Mel-18* 3′ untranslated region was amplified from genomic DNA. The PCR primer sequences were 5′-TGCTGTCCTGCCTCTGACCAGT-3′ and 5′-CTCAGAACCAGGGATAAACTGCAT-3′. The PCR reactions were performed as described previously.[17] Digestion of the fragment with HpyCH4IV resulted in two fragments of 70 and 40 bp for the *A allele*, and a 110 bp fragment for the *G allele* (Supporting Information Fig. 1). These genotypes were confirmed using GENESCAN software (Applied Biosystems, Foster City, CA).

Measurement of 1805A/G expression of Mel-18

The cDNA from seven cell lines heterozygous for the *1805A/G* polymorphism, including DU145, NC65, CCFRC1, 253J, TCCSUP, 5637 and KU7, was subjected to PCR using primers from the TaqMan® SNP Genotyping Assay kit (ABI Applied Biosystems). The real-time intensity of fluorescence (VIC for 1805*G* and FAM for 1805*A*) was measured using the TaqMan® Gene Expression Master Mix (ABI Applied Biosystems).

Real-time quantitative RT-PCR

The transcriptional levels of *Mel-18*, Bmi-1, c-Myc, and an endogenous control gene (*GAPDH*) were analyzed using the Thermal Cycler Dice™ Real Time System (Takara) with their respective gene specific quantitative real-time RT-PCR primers (Supporting Information Table I), as described previously.[7]

Statistical analysis

Hardy-Weinberg equilibrium analyses were performed to compare the observed genotype frequencies of each category with the expected frequencies using a Chi-square test (degrees of freedom = 1). The age-adjusted odds ratio (aOR) and 95% confidence interval (CI) for the relative risk of prostate cancer and the relationship between the Mel-18 expression or the genotype and histological or clinical variables were determined by multivariate logistic regression analysis with the inclusion of age as a factor. Correlation between gene expression levels was examined using the Spearman coefficient. The survival time was calculated from the date of prostate cancer diagnosis to the date of prostate specific antigen (PSA) recurrence, death from prostate cancer, or death from any cause, for PSA recurrence-free, cancer-specific, and overall survival, respectively. PSA recurrence was defined as the persistence of a post-operative serum PSA level >0.4 ng/ml. PSA recurrence free, cancer-specific, and overall survival were estimated using the Kaplan-Meier method and significant differences in survival were tested using the log rank test. Hazard ratios (HRs) and 95% CIs for cancer death were assessed by the Cox proportional hazard regression model. All of the data were entered into an access database and analyzed using the Excel 2000 or SPSS

TABLE I – CORRELATION BETWEEN MEL-18 EXPRESSION AND CLINICOPATHOLOGICAL FEATURES

Variables	Overall	Mel-18 expression				
		Negative (%)	Positive (%)	*p* Value	Staining score	*p* Value
Overall	131	56 (42.7)	75 (57.3)		5.5 ± 4.2	
Clinical factor						
Age (year)						
−60	14	6 (42.9)	8 (57.1)	0.632	6.2 ± 4.9	0.728
61–70	50	22 (44.0)	28 (56.0)		5.7 ± 4.5	
71–80	61	24 (39.3)	37 (60.7)		5.2 ± 3.8	
81–	6	4 (66.7)	2 (33.3)		4.3 ± 3.6	
PSA (ng/mL)						
0.0–10.0	61	20 (32.8)	41 (67.2)	0.004	6.4 ± 4.4	0.007
10.1–20.0	39	16 (41.0)	23 (59.0)		5.7 ± 4.2	
20.1–100.0	20	10 (50.0)	10 (50.0)		3.9 ± 2.8	
100.1–	11	10 (90.9)	1 (9.1)		2.5 ± 2.3	
Pathological factor						
Pathological stage						
T2N0M0	70	29 (41.4)	41 (58.6)	0.017	6.1 ± 4.6	0.027
T3N0M0	39	12 (30.8)	27 (69.2)		5.5 ± 3.9	
T4< or N1 or M1	22	15 (68.2)	7 (31.8)		3.4 ± 2.3	
Primary Gleason grade						
2,3	65	21 (32.3)	44 (67.7)	0.044	6.3 ± 4.6	0.139
4	53	27 (50.9)	26 (49.1)		4.9 ± 3.7	
5	13	8 (61.5)	5 (38.5)		4.5 ± 3.4	
Gleason score (primary grade + secondary grade)						
5–6	22	4 (18.2)	18 (81.8)	0.023	7.2 ± 5.0	0.026
7	62	27 (43.5)	35 (56.5)		5.8 ± 4.5	
8–10	47	25 (53.2)	22 (46.8)		4.4 ± 3.0	
5–6, 7 (3 + 4)	56	20 (32.8)	41 (67.2)	0.031	6.6 ± 5.0	1.631e-005
7 (4 + 3), 8–10	75	36 (51.4)	34 (48.6)		4.6 ± 3.2	
5–8	99	37 (37.4)	62 (62.6)	0.029	6.0 ± 4.4	0.034
9, 10	32	19 (59.4)	13 (40.6)		4.2 ± 3.1	

(version 10.0J; SPSS, Inc.) software. A probability value of $P < 0.05$ was considered to be statistically significant.

Results

Mel-18 expression and clinical and pathological variables in prostate cancer tissues

First, we examined Mel-18 expression in prostate cancer tissues by immunohistochemistry. In the normal prostatic gland epithelium, strong expression was seen in the nucleus, whereas staining in the cytoplasm was minimal (Figs. 1*a,b*). In contrast, nuclear staining varied among the prostate cancer tissue samples. Typically diminished nuclear expression was frequent in high grade prostate cancer tissues, whereas relatively strong nuclear expression was observed in low grade prostate cancers (Fig. 1*c–h*). In order to clarify the relationship between the clinical and pathological variables and Mel-18 expression, we quantified Mel-18 expression in prostate cancer tissues.

Using immunohistochemistry, we found that histologically low grade and clinically low stage prostate cancers demonstrated significantly higher Mel-18 expression than high grade and high stage cancers (Table I). Significant differences in the Mel-18 staining score relative to serum levels of PSA, pathological stages, and Gleason scores of the patients were detected (Table I). Moreover, patients with positive Mel-18 expression ($n = 75$) had significantly longer PSA recurrence-free survival after radical prostatectomy than patients negative for Mel-18 expression ($n = 56$, $p = 0.038$, Fig. 1*i*).

The mRNA expression of different Mel-18 alleles

We found a *1805A/G* SNP, located in the 3′ untranslated region of *Mel-18* using the NCBI SNP database. The *1805A/G* SNP is predicted to be located at a putative miR-181a binding site by the microRNA binding site prediction software, miRNA Targets (Fig. 2*a*). In addition, according to MFOLD, the mRNA secondary structure prediction tool, the putative secondary structures of the *G* and *A* alleles of *1805A/G Mel-18* differ considerably (Fig. 2*b*).

The *A/G* substitution causes an obvious change in the mRNA, suggesting that this alteration could cause differences in the mRNA stability or protein-translation efficiency (Fig. 2*b*). Therefore, we investigated the expression of each of these *Mel-18* alleles. We used seven urological cancer cell lines, which have a heterozygous *GA* genotype at the *1805A/G* SNP, as described in Material and methods. We found that expression of the *1805A* allele was significantly higher than the *1805G* allele in the seven urological cancer cell lines (Fig. 2*c*) although the expression ratio of *1805A* to *1805G* in the genomic DNA from these heterozygous cell lines was similar (Fig. 2*d*).

Association between the 1805A/G Mel-18 genotype and the risk of prostate cancer

Because the *A* and *G* alleles of *Mel-18* exhibited different levels of expression, we examined the association between the *Mel-18* polymorphism and the risk of prostate cancer. The observed genotype frequency of the polymorphism did not differ from the expected frequency according to the Hardy-Weinberg equilibrium in the control group (data not shown).

The genotype distribution of the *Mel-18 1805A/G* polymorphism is summarized in Table IIA and IIB. There was no significant difference in the genotype distribution between the control and prostate cancer groups (Table IIA). Age-adjusted logistic regression analysis showed no association between the SNP genotype and the risk of prostate cancer (Table IIA). In this genotype analysis, however, we found that the distribution of the *AA* genotype was significantly higher in histologically low or intermediate grade and clinically localized prostate cancers than in the high grade and metastatic cancers (Table IIB).

The association between the Mel-18 polymorphism and cancer progression after radical prostatectomy

Next, we examined the association between the *Mel-18* polymorphism and cancer progression after radical prostatectomy. The

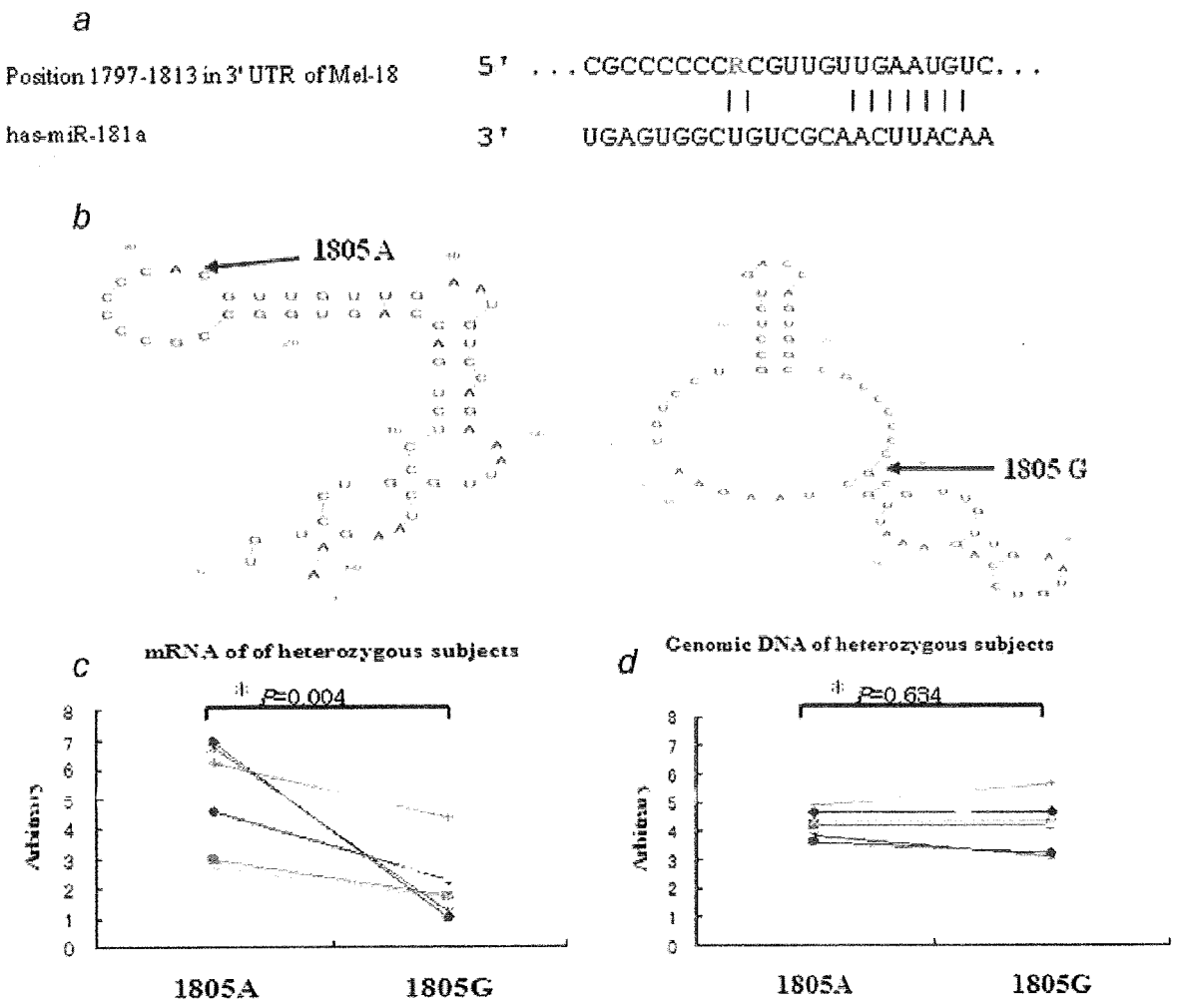

FIGURE 2 – *Mel-18 1805A/G* polymorphism and clinical significance. (*a*) The *Mel-18* 3′ UTR contains a miR-181a binding site. Schematic microRNA binding site structures for the *1805A/G* alleles. (*b*) *Mel-18* mRNA folding structures predicted by MFOLD. (*c*) The mRNA expression for the *1805A* and *1805G* alleles in the *1805A/G* heterozygous cell lines including DU145, NC65, CCFRC1, 253J, TCCSUP, 5637, and KU7. (*d*) Quantitation of the control products amplified from genomic DNA (*$p = 0.004$). [Color figure can be viewed in the online issue, which is available at www.interscience.wiley.com.]

mean age ± SD of the 124 patients who underwent radical prostatectomy was 70.2 ± 5.1 years. The mean follow-up period was 36.3 ± 22.8 months. The mean preoperative serum PSA was 17.0 ± 14.9 ng/ml.

The distribution of clinical stages of these patients, T1, T2, and T3 was 45 (36.3%), 58 (46.8%) and 21 (16.9%), respectively. The distribution of pathological stages, pT2, pT3, and pT4 was 73 (58.9%), 43 (34.7%), and 8 (6.5%), respectively, and a positive surgical margin was observed in 76 (61.3%) cases. A Gleason sum score of <7, 7, and >7 was present in 25 (20.2%), 52 (41.9%) and 47 (37.9%), respectively. The 3- and 5-year PSA recurrence-free survival rates were 66.8% and 37.9%, respectively, with a median survival time of 58.1 months. Kaplan-Meier survival curves stratified by *Mel-18* genotype demonstrated that patients with the *GG* genotype had a significantly higher rate of PSA recurrence compared to the *AA* or *GA* genotype ($p = 0.002$, Fig. 3*a*).

Univariate analysis of the PSA recurrence-free survival stratified by dichotomized groups for each factor showed that PSA = 9.6 ($p = 0.003$), pathological T status =T3 ($p < 0.001$), positive surgical margin ($p < 0.001$), the *GG* genotype ($p = 0.004$), and negative Mel-18 expression ($p = 0.042$) were each significantly associated with poor survival (Table IIIA). In a multivariate analysis, higher PSA level, positive surgical margin, the presence of the *GG* genotype, and negative Mel-18 expression were independent risk factors predicting PSA recurrence after radical prostatectomy, with HRs of 3.095 (95% CI, 1.352–7.083; $p = 0.007$), 4.759 (95% CI, 1.857–12.191; $p = 0.001$), 2.757 (95% CI, 1.154–6.588; $p = 0.022$) and 2.271 (95% CI, 1.018–5.066; $p = 0.045$), respectively (Table IIIA).

Association between the Mel-18 polymorphism and survival in patients with metastatic prostate cancer

Next, we examined the association between the *Mel-18* polymorphism and survival of metastatic prostate cancer patients. The mean age ± SD of the 66 patients with bone metastases at diagnosis was 72.6 ± 8.5 years. The mean follow-up period was 53.3 ± 38.9 months. The 5-year overall survival rates were 52.2 months, with a median survival time of 64.8 months.

Survival was compared between the two groups divided according to the *Mel-18* genotype, *i.e.*, patients with the *AA*

TABLE II – GENOTYPE FREQUENCIES OF THE MEL-18 SNPS AND AGE-ADJUSTED ODDS RATIO

Mel-18 1805A/G Genotype	Male controls *n* (%)	Prostate cancer *n* (%)	aOR[1] (95% CI[2])	*p*
(A) Comparison of prostate cancer patients with male controls				
Mel-18 1805 A/G	146	393		
AA	71 (48.6%)	170 (43.3%)	ref	
GA	60 (41.1%)	179 (45.5%)	1.254 (0.837–1.879)	0.273
GG	15 (10.3%)	44 (11.2%)	1.238 (0.642–2.362)	0.532
GA + *GG* (against *AA*)	75 (51.4%)	223 (56.7%)	1.248 (0.851–1.830)	0.256
GA + *AA* (against *GG*)	131 (89.7%)	349 (88.8%)	0.907 (0.487–1.690)	0.758
Mel-18 1805A/G Genotype	Stage[3]		aOR[1] (95% CI[2])	*p*
	Localized	Metastatic		
(B) Comparison of patients with high stage or high grade prostate cancers to patients with low stage or low grade prostate cancers				
AA	139 (47.4%)	31 (31.0%)	ref	
GA	126 (43.0%)	53 (53.0%)	1.792 (1.071–2.999)	0.026
GG	28 (9.6%)	16 (16.0%)	2.409 (1.148–5.058)	0.020
GA + *GG* (against *AA*)	154 (52.6%)	69 (69.0%)	1.906 (1.166–3.115)	0.010
GA + *AA* (against *GG*)	265 (90.4%)	84 (84.0%)	0.573 (0.292–1.126)	0.106
Mel-18 1805A/G Genotype	Grade[4]		aOR[1] (95% CI[2])	*p*
	Low + Intermediate	High		
AA	108 (47.0%)	57 (36.3%)	ref	
GA	101 (43.9%)	77 (49.0%)	1.517 (0.971–2.371)	0.067
GG	21 (9.1%)	23 (14.6%)	2.272 (1.146–4.508)	0.019
GA + *GG* (against *AA*)	122 (53.0%)	100 (63.7%)	1.646 (1.076–2.517)	0.022
GA + *AA* (against *GG*)	209 (90.9%)	134 (85.4%)	0.549 (0.289–1.041)	0.066

[1]Age-adjusted odds.–[2]95% confidence interval. –[3]Localized, stage A–C; metastatic, stage D.–[4]Low, well-differentiated or Gleason score 2–4; intermediate, moderately differentiated or Gleason score 5–7; High, poorly differentiated or Gleason score 8–10.

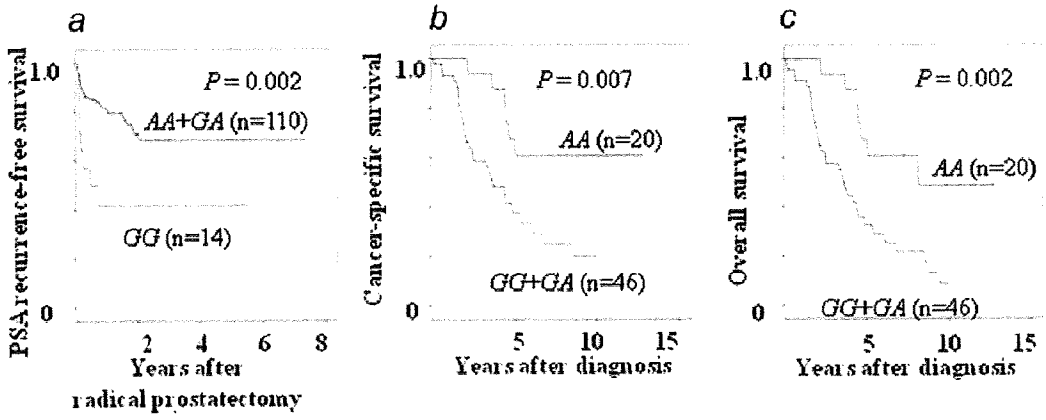

FIGURE 3 – Association between the *Mel-18* polymorphism and survival in patients with prostate cancer. Kaplan-Meier curves of PSA recurrence-free survival in patients with prostate cancer who underwent radical prostatectomy (*a*). Kaplan-Meier curves of cancer-specific survival (*b*) and overall survival (*c*) in patients with prostate cancer and bone metastasis at initial diagnosis. [Color figure can be viewed in the online issue, which is available at www.interscience.wiley.com.]

genotype (n = 20) and with the *GA* or *GG* genotype (n = 46). The *AA* genotype was associated with significantly better cancer-specific and overall survival compared with the *GA* or *GG* genotype (p = 0.007 and p = 0.002, respectively; Fig. 3*b* and 3*c*). The 5-year overall survival rates were 48.3% for patients with the *GA* or *GG* genotype and 69.2% for patients with the *AA* genotype. The median cancer-specific survival time of patients with the *GA* or *GG* genotype was 46.9 months and with the *AA* genotype 81.6 months. The median overall survival time of patients with the *GA* or *GG* genotype was 48.9 months and with the *AA* genotype was 76.9 months.

In a univariate analysis, age (p = 0.044), pretreatment PSA level (p = 0.002), levels of hemoglobin (p < 0.001), alkaline phosphatase (p < 0.001), and lactate dehydrogenase (p = 0.030), as well as *Mel-18* polymorphism (p = 0.011), were significantly associated with cancer-specific survival. A multivariate analysis revealed that the Mel-18 *A* allele (p = 0.019), elevated serum PSA (p = 0.037), and elevated serum alkaline phosphatase (p < 0.001) were independent predictors of poor cancer-specific survival (Table IIIB).

Mel-18 expression and the Mel-18 1805A/G genotypes

We examined the association between Mel-18 expression and *Mel-18 1805A/G* genotype in patients with prostate cancer. The patients with the *Mel-18* 1805 *AA* genotype tended to have higher

TABLE III – COX PROPORTIONAL HAZARD REGRESSION ANALYSIS OF PREDICTING FACTORS FOR PSA RECURRENCE-FREE SURVIVAL IN PROSTATE CANCER PATIENTS WHO UNDERWENT RADICAL PROSTATECTOMY (A) AND IN PATIENTS WITH BONE METASTASIS (D2) AT DIAGNOSIS (B)

Variable	Category for statistical analysis	PSA recurrence-free survival		
		HR[1]	95% CI[2]	*p*
(A)				
Univariate analysis				
Preoperative PSA	≥9.6 *vs.*<9.6 (ng/ml)	2.643	1.377–5.074	0.003
Pathological T status	T3-4 *vs.* T2	3.934	2.065–7.493	<0.001
Surgical margin status	Positive *vs.* Negative	3.637	1.876–7.050	<0.001
Gleason Score	≥8 *vs.*<8	1.348	0.731–2.485	0.399
Mel-18 polymorphism	*GG vs. AA/GA*	3.222	1.458–7.120	0.004
Immuohistochemical staining of Mel-18	<4 *vs.*≥4	2.013	1.025–3.955	0.042
Multivariate analysis				
Preoperative PSA	≥9.6 *vs.*<9.6 (ng/ml)	3.095	1.352–7.083	0.007
Pathological T status	T3-4 *vs.* T2	1.311	0.5528–3.188	0.540
Surgical margin status	Positive *vs.* Negative	4.759	1.857–12.191	0.001
Mel-18 polymorphism	*GG vs. AA/GA*	2.757	1.154–6.588	0.022
Immuohistochemical staining of Mel-18	<4 *vs.* ≥4	2.271	1.018–5.066	0.045
Variable	Category for statistical analysis	Cancer-specific survial		
		HR[1]	95% CI[2]	*p*
(B)				
Univariate analysis				
Age	≥71 *vs.* <71 (yrs)	1.899	1.018–3.542	0.044
Tumor grade	High *vs.* Low/Intermediate	1.097	0.598–2.012	0.764
PSA	≥176 *vs.*<176 (ng/ml)	2.823	1.484–5.370	0.002
Hemoglobin	<11.5 *vs.* ≥11.5 (g/dl)	15.790	5.304–47.006	<0.001
Alkaline phosphatase	Increased *vs.* Normal	3.623	1.832–7.165	<0.001
Lactate dehydrogenase	Increased *vs.* Normal	2.319	1.086–4.956	0.030
Mel-18 polymorphism	*GG/GA vs. AA*	3.165	1.304–7.685	0.011
Multivariate analysis				
Age	≥71 *vs.* <71 (yrs)	1.212	0.442–3.321	0.709
PSA	≥176 *vs.* <176 (ng/ml)	2.825	1.122–7.110	0.027
Hemoglobin	<11.5 *vs.* ≥11.5 (g/dl)	1.973	0.317–12.268	0.466
Alkaline phosphatase	>ULN *vs.* Normal	27.093	4.676–156.970	<0.001
Lactate dehydrogenase	>ULN *vs.* Normal	1.427	0.391–5.199	0.590
Mel-18 polymorphism	*GG/GA vs. AA*	4.658	1.287–16.858	0.019

[1]HR: hazard ratio.–[2]CI: confidence interval.–[3] ULN, upper limits of the normal range.

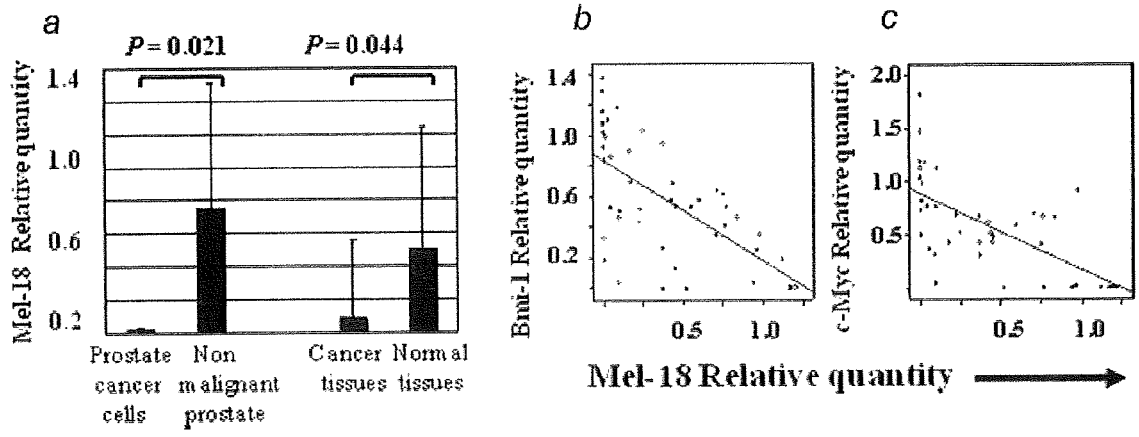

FIGURE 4 – Comparison of relative Mel-18 expression. Comparison of Mel-18 expression between prostate cancer cell line and non-malignant prostate tissues (left side), and between the renal and bladder cancer tissues and surrounding normal tissues (*a*). Correlation between *Mel-18* and *Bmi-1* expression in the malignant and non-malignant tissues (*b*). Correlation between *Mel-18* and c-*Myc* expression in the malignant and non-malignant tissues (*c*).

Mel-18 expression than those with *GA* or *GG* genotypes although the difference was not statistically significant ($p = 0.188$). Other confounding factors such as promoter activity or modulation by microRNAs may modify Mel-18 expression in prostate cancer tissues.

Finally, we examined the expression levels of *Mel-18*, *Bmi-1*, and *c-Myc* mRNA in 2 prostate cancer cell lines, PC-3 and DU145, 12 non-cancerous prostate tissues, 7 renal cancers and the surrounding non-cancerous tissues, and 8 bladder cancers and the surrounding non-cancerous tissues. Using quantitative real time-

RT-PCR, *Mel-18* mRNA levels in prostate cancer cell lines were significantly lower than those in non-cancerous prostate tissues (Fig. 4*a*). We also found that levels of *Mel-18* mRNA in renal and bladder cancer tissues were significantly lower than those in surrounding non-cancerous tissues (Fig. 4*a*). In addition, statistically significant direct correlations were observed between levels of expression of *Mel-18* and *Bmi-1* and *c-Myc*, in all samples. A strong negative correlation was observed between *Mel-18* and *Bmi-1* ($r = -0.678$, $p < 0.001$) and between *Mel-18* and *c-Myc* ($r = -0.670$, $p < 0.001$) (Figs. 4*b,c*).

Discussion

Our immunohistochemical and clinicopathological data are consistent with the hypothesis that Mel-18 functions as a tumor suppressor protein in prostate cancer and possibly represses expression of the oncoproteins, c-Myc and Bmi-1. These observations are also consistent with previous examinations of prostate and breast cancer cells.[8,9] Because of the difficulty in comparing inter-institutional evaluations, immunohistochemical evaluation is often not clinically useful. Therefore, we sought an alternative method of investigating the association between *Mel-18* and prostate cancer. Our study demonstrated a *Mel-18* allele with low expression, the *1805 G* allele, was correlated with risk not only for poorer survival rates of patients with localized prostate cancer, but also with a poor prognosis in patients with metastatic prostate cancer. In this study, we examined Mel-18 gene expression corresponding to each allele of the *1805A/G* polymorphism in the prostate and in other cancer cell lines and found that the expression of the *1805A* allele was consistently higher than the *1805G* allele in seven cancer cell lines (Figs. 2*c,d*). Since we examined differences in the allelic mRNA expression in individual cancer cell lines from heterozygous subjects, the effects of environmental and/or other non-genetic factors would be exclude. In this study, the patients with the patients with the *GG* genotype had a significantly higher rate of PSA recurrence after prostatectomy compared to the *AA* or *GA* genotype ($p = 0.002$, Fig. 3*a*), whereas the *GG/GA* genotypes were associated with significantly worse cancer-specific and overall survival of the patients with metastasis compared with the *AA* genotype ($p = 0.007$ and $p = 0.002$, respectively; Fig. 3b and 3*c*). The sensitivity to hormonal and/or chemotherapeutic treatments might modify the survival of the metastatic prostate cancer patients.

Recent studies have provided evidence that SNPs in microRNA-binding sites in the 3′ untranslated region of tumor associated genes may be important factors for cancer risk.[19–21] The microRNA–RNA silencing complexes can inhibit translation when the microRNA binds to the 3′ untranslated-region (UTR)-mRNA target with an imperfect complementarity. This binding results in a reduced level of protein without reductions in the mRNA level.[22,23] In our study, the miRNA181a and 3′ UTR of the *Mel-18* showed an imperfect complementarity. However, the mRNA levels of the respective alleles demonstrated significant differences, suggesting that this altered expression may result from some as yet unidentified mechanism. Alterations in the 3' UTR can also affect the stability of an mRNA due to increased sensitivity to RNase. Partial folding structures of the *1805G* and *1805A* mRNAs, predicted by MFOLD, are shown in Figure 2*b*. These clearly different secondary structures may suggest that the different mRNAs differ in their protein-translational efficiencies.

Mel-18 is structurally highly similar to *Bmi-1*, another PcG member whose over-expression has been linked to the highly malignant behavior of various cancer cells including prostate cancer.[5,6] The N-terminal region of *Mel-18*, which contains a RING finger domain, is 93% homologous to the corresponding region of Bmi-1.[7] *Bmi-1* is negatively regulated by *Mel-18 via* repression of the *c-Myc* oncogene, which is amplified and/or overexpressed in a variety of malignancies.[8–11] Recent genome-wide analysis has identified variants in five chromosomal regions, including three independent regions, 8q24, 17q12, and 17q24.3, that are significantly associated with prostate cancer.[12,13] Although we failed to demonstrate an association between the *Mel-18 1805A/G* polymorphism and a risk of prostate cancer, prostate cancer is a slow growing cancer with a long period between initiation and formation of a clinically significant cancer, suggesting that progression rather than initiation may be the rate-limiting factor in the diagnosis of clinical cancer. In addition, *c-Myc*, whose chromosomal location is at 8q24, regulates androgen-receptor mediated transcriptional signals and may also function in oncogenesis of prostate cancer.[24] In a breast cancer study, *Bmi-1* and *c-Myc* were transcriptionally repressed by *Mel-18*.[10,11] This observation is consistent with our study, where we found a significant negative correlation between the expression of *Mel-18* and *c-Myc* in prostate cancer. Further investigation will be necessary to understand the association between these *Mel-18* mediated tumor-suppressive and *c-Myc* mediated oncogenic signals in prostate cancer.

In conclusion, our study, together with recent research on Mel-18 in various cancers, suggests that Mel-18 functions as a tumor suppressor in prostate cancer. To our knowledge, this is the first study to evaluate the association among Mel-18 expression and genotype, and the clinical significance thereof, for patients with prostate cancer. We recognized, however, that no correction was made for multiple testing in the p values reported for genotype association and that this observation requires independent replication. Although further studies using other validation methods will be necessary to confirm the involvement of Mel-18 in the progression of prostate cancer, the present study provides important evidence indicating that Mel-18 is a possible therapeutic target, as well as a diagnostic marker for poor outcome in prostate cancer patients.

Acknowledgements

The authors thank Yoko Mitobe, Yuka Izumida and Tomomi Kawamura for their technical assistance.

References

1. Sparmann A, van Lohuizen M. Polycomb silencers control cell fate, development and cancer. Nat Rev Cancer 2006;6:846–56.
2. Raaphorst FM. Self-renewal of hematopoietic and leukemic stem cells: a central role for the Polycomb-group gene Bmi-1. Trends Immunol 2003;24:522–4.
3. Dirks P. Bmi1 and cell of origin determinants of brain tumor phenotype. Cancer Cell 2007;12:295–7.
4. Glinsky GV. "Stemness" genomics law governs clinical behavior of human cancer: implications for decision making in disease management. J Clin Oncol 2008;26:2846–53.
5. Glinsky GV, Berezovska O, Glinskii AB. Microarray analysis identifies a death-from-cancer signature predicting therapy failure in patients with multiple types of cancer. J Clin Invest 2005;115:1503–21.
6. Mohty M, Yong AS, Szydlo RM, Apperley JF, Melo JV. The polycomb group BMI1 gene is a molecular marker for predicting prognosis of chronic myeloid leukemia. Blood 2007;110:380–3.
7. Goebl MG. The bmi-1 and mel-18 gene products define a new family of DNA-binding proteins involved in cell proliferation and tumorigenesis. Cell 1991;66:623.
8. Kanno M, Hasegawa M, Ishida A, Isono K, Taniguchi M. mel-18, a Polycomb group-related mammalian gene, encodes a transcriptional negative regulator with tumor suppressive activity. EMBO J 1995; 14:5672–8.
9. Silva J, García JM, Peña C, García V, Domínguez G, Suárez D, Camacho FI, Espinosa R, Provencio M, España P, Bonilla F. Implication of polycomb members Bmi-1, Mel-18, and Hpc-2 in the regulation of p16INK4a, p14ARF, h-TERT, and c-Myc expression in primary breast carcinomas. Clin Cancer Res 2006;12:6929–36.
10. Guo WJ, Zeng MS, Yadav A, Song LB, Guo BH, Band V, Dimri GP. Mel-18 acts as a tumor suppressor by repressing Bmi-1 expression and down-regulating Akt activity in breast cancer cells. Cancer Res 2007;67:5083–9.